IEEE Access
Multidisciplinary ⋮ Rapid Review ⋮ Open Access Journal

Received 23 February 2026, accepted 24 March 2026, date of publication 1 April 2026, date of current version 10 April 2026.

Digital Object Identifier 10.1109/ACCESS.2026.3679804

TOPICAL REVIEW

Integrated On-Board Chargers for Electric Vehicles: Topologies, Control Strategies, Challenges, and Future Research Directions

MALIK QAMAR ABBAS[1], (Student Member, IEEE), LASSI AARNIOVUORI[2], (Senior Member, IEEE), PASI PELTONIEMI[2], (Senior Member, IEEE), MICHELE MENGONI[1], (Senior Member, IEEE), AND LUCA ZARRI[1], (Senior Member, IEEE)

[1]Department of Electrical, Electronic, and Information Engineering "Guglielmo Marconi," University of Bologna, 40136 Bologna, Italy
[2]LUT School of Energy Systems, 53850 Lappeenranta, Finland

Corresponding author: Lassi Aarniovuori (Lassi.Aarniovuori@lut.fi)

ABSTRACT The rapid adoption of electric vehicles (EVs) is increasing the demand for charging solutions that are compact, cost-effective, and grid-friendly. Conventional off-board charging stations face challenges such as high infrastructure cost, distribution-grid stress from high-power charging, and limited flexibility for RE integration. Integrated on-board chargers (IOBCs) offer a promising alternative by reusing the traction inverter and motor for charging, thereby reducing system size, weight, and cost, while improving hardware utilization. Despite growing research interest, a consolidated and critical assessment of IOBC architectures and control strategies remains limited. This paper presents a comprehensive review of IOBC technologies, covering key topologies and control approaches for charging, traction, and vehicle-to-grid (V2G) operation. It critically examines major implementation challenges, including unintended charging torque and torque ripple, harmonic current distortion and grid-code compliance, thermal stress due to high power density, and safety and isolation constraints. Finally, future research directions are discussed, with an emphasis on advanced converter topologies, wide-bandgap devices, enhanced thermal management, cybersecurity, and data-driven resilience for secure and reliable EV charging systems.

INDEX TERMS Charging station, charging topologies, electric vehicles, integrated on-board charger, multiphase machine.

I. INTRODUCTION

The Intergovernmental Panel on Climate Change (IPCC) identifies climate change as a major global challenge, necessitating immediate reductions in greenhouse gas emissions in all sectors [1]. According to the International Energy Agency (IEA), the transportation sector alone accounts for 24% the production of carbon dioxide in the atmosphere [2]. In the US alone, the transportation sector contributes the highest percentage of greenhouse gas emissions, as demonstrated in Fig. 1 [3]. Among direct transport emissions, road transportation is the dominant source, contributing around 70%, followed by aviation (12%), shipping (11%), and rail (1%) [4]. Road transportation includes a large number of heavy-duty commercial vehicles and a few percent of battery-based electric vehicles (EVs), i.e., 2.5%. To reduce the transportation sector's dependence on conventional internal combustion engines, EV sales have increased significantly over the past decade. In the first quarter of 2023, there appear to be 140% more EV sales than in the same period in 2024. As shown in Fig. 2, Asia Pacific leads the sales market with approximately 700,000 EVs sold in 2024.

The associate editor coordinating the review of this manuscript and approving it for publication was Minh C. Ta.

© 2026 The Authors. This work is licensed under a Creative Commons Attribution 4.0 License.
For more information, see https://creativecommons.org/licenses/by/4.0/

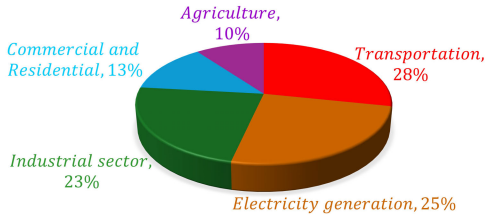

FIGURE 1. Total U.S. greenhouse gas emissions in 2022 [3].

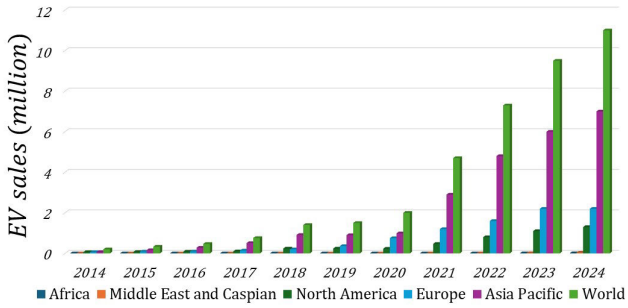

FIGURE 2. Global EV sales between, 2014-2024 [5].

Europe follows with 200,000 units sold, while sales in the United States appear to have doubled compared to the first quarter of 2022 [5]. Despite the growing market adoption of EVs, their widespread deployment remains constrained by several factors, including high cost, limited driving range, inadequate charging infrastructure, and long charging times. Although the driving range can be improved by increasing battery capacity, the battery itself accounts for nearly 50% of the total EV cost. Consequently, increasing battery capacity to extend range results in higher vehicle prices and larger physical dimensions, thereby limiting the practicality of this approach [6]. However, researchers are actively developing charging stations that are cost-effective, simple in design, easily accessible, capable of fast charging, and supportive of extended driving range. Based on voltage, current, power, and the nature of the voltage (DC/AC), SAEJ1772 standardized three levels for charging stations: level 1, level 2, and level 3, as demonstrated in Table 1 [7], [8]. Levels 1 and 2 are for slow charging, with charging times of the whole night and AC voltages of 230 and 400 V, respectively. On the other hand, levels 3 and 4 correspond to fast and extremely fast chargers with DC voltages ranging from 400 to 1000 V.

There are two types of EV chargers based on the location of the charging circuitry: on-board chargers, which have their circuitry inside the vehicle, and off-board chargers, which have it outside the vehicle [7], [10], [11]. Off-board charging stations can surely reduce charging time and improve the range of commercial EVs, but with the huge cost of operation, installation, and integration due to their high-density power (>350 kW) [10], [12], [13]. In addition, off-board charging stations are not easily found everywhere. So, all these constraints motivate researchers to investigate on-board EV chargers, which are surely less costly, simpler, lighter, and, more importantly, readily available [14], [15], [16]. However, on-board chargers (OBCs) take longer to charge vehicles due to their limited power-transfer capacity, constrained by size, volume, and weight [17], [18]. To avoid separate power-electronics circuits for charging and traction, the concept of an Integrated OBC (IOBC) emerged, which uses the same power converters, motor circuit, and power inverter for both charging and propulsion, since these processes do not occur simultaneously [19]. Different types of battery chargers are shown in Fig. 3. In IOBCs, the motor stator windings act as a filter inductance for the current ripples from the grid, and the voltage source inverter works as a bidirectional converter for both charging and propulsion purposes [20], [21]. Such integrated chargers can transfer power from grid to vehicle (G2V), vehicle to grid (V2G), vehicle to vehicle (V2V), and from vehicle to other devices having their bidirectional power converter and active front-end Power Factor Correction (PFC) converter [14], [22], [23]. Some challenges arise when adopting powertrain components for both charging and propulsion stages, such as unnecessary torque during charging, torque and current ripples, thermal stress, isolation and safety issues, and electromagnetic interference (EMI) [24], [25].

Unwanted rotor movement during charging occurs when currents flowing through the machine windings generate electromagnetic torque even in the absence of commanded propulsion, potentially causing mechanical stress on drivetrain components and posing safety risks to the vehicle and its surroundings [26]. To mitigate charging torque and associated torque ripple, the literature proposes solutions at multiple levels, including control-based torque cancellation, topology-level winding reconfiguration, and machine-level design modifications. In parallel, switching actions of power electronic devices, pulsating winding currents, zero-sequence circulating currents, phase interactions, and imperfect decoupling between propulsion and charging states introduce harmonic distortion and current ripple, increasing copper and core losses and degrading grid-side power quality, necessitating compliance with grid codes and harmonic standards. The push toward high-power-density IOBCs further intensifies the thermal management challenges due to elevated current levels, higher switching frequencies, and compact packaging, which restrict conventional cooling approaches and demand efficient thermal design. Additionally, isolation and safety requirements impose stringent constraints on IOBC architectures, as adequate electrical isolation between the grid, battery, and vehicle chassis, along with proper grounding, insulation coordination, and fault detection, is essential for safe operation under both normal and fault conditions. Therefore, a comprehensive and systematic analysis is required to address these interrelated challenges during IOBC operation [27], [28], where the

TABLE 1. Characteristics of different charging levels of EV chargers [7], [8].

Charging level	Power rating	Current rating	Charging time (hours)	Range (miles)	Charger location
Level 1 (Single-phase) 120 Vac (US) 230 Vac (EU)	3.7 kW	12-16 A	10-15	5	Residential
Level 2 (Single-phase or three-phase) 240 Vac (US) 400 Vac (EU)	3.7–22 kW	15–80 A	3.5-7	10–20	Private or commercial outlets
Level 3 (Three-phase) 208 Vac 600 Vdc	50–350 kW	up to 400 A	0.16–0.5	$>$ 75	Private or commercial outlets
Level 4 (Extremely Fast DC Charging Station) 1000 Vdc and above	$>$ 400 kW	$>$ 400 A	0.16 approx	$>$ 100	Private or commercial outlets

TABLE 2. Comparison among the performance of different types of electric motors [9].

Condition and Aspect	PMSM	BLDC	SRM	IM	SynRM
Starting	High starting torque with smooth startup	Efficient start with no high inrush current	High starting torque but with torque pulsations	Low starting torque with high load capacity	Moderate starting torque, requires assisted starting
Low-speed operation in different quadrants (I, II, III, IV)	Shows best efficiency with high starting torque and low ripples (I)	Good efficiency and smooth operation (II)	High torque with vibration (IV)	Less efficient with high slip (III)	Moderate efficiency, torque ripple present (III)
Speed range	Wide speed range with high efficiency (I)	Limited range with medium efficiency (III)	Moderate range with less stability (II)	Narrow range with reduced efficiency (IV)	Wide speed range but lower efficiency than PMSM
Cost	High	High	Medium	Low	Medium
Size	Small	Small	Large	Medium	Medium
Pros	High efficiency with smooth torque	Compactness with low maintenance and high efficiency	High starting torque with no rare-earth and medium efficiency	Robust, cost-effective with low efficiency	Robust, magnet-free, low cost, suitable for medium/high-speed drives
Cons	Expensive with rare-earth materials	Torque oscillations with limited high-speed performance	High noise with torque ripples	Low efficiency with more slip loss	Lower efficiency than PMSM, torque ripple, requires advanced control

selection of the traction motor and its electromagnetic characteristics plays a decisive role in determining torque behavior, harmonic sensitivity, and the feasibility of achieving torque-free charging. Consequently, a clear understanding of the available traction motor technologies is essential, as each motor type exhibits distinct electromagnetic characteristics that directly influence IOBC performance and operational constraints.

The different types of motor used in EVs are classified as Induction Motor (IM), Switched Reluctance Motor (SRM), and Synchronous Motor, which can be further divided into Permanent Magnet Synchronous Motors (PMSM), Externally Excited Synchronous Motors (EESM), and Synchronous Reluctance Motor (SynRM). The comparison of different types of motors used in EVs is shown in Table 2. Based on this comparison, it can be deduced that PMSM has a high torque capacity, high efficiency, high power density, and stability compared to other motor types [9], [29], [30]. Similarly, IM has high reliability, low cost, high controllability, and high overload capacity [31], [32], [33].

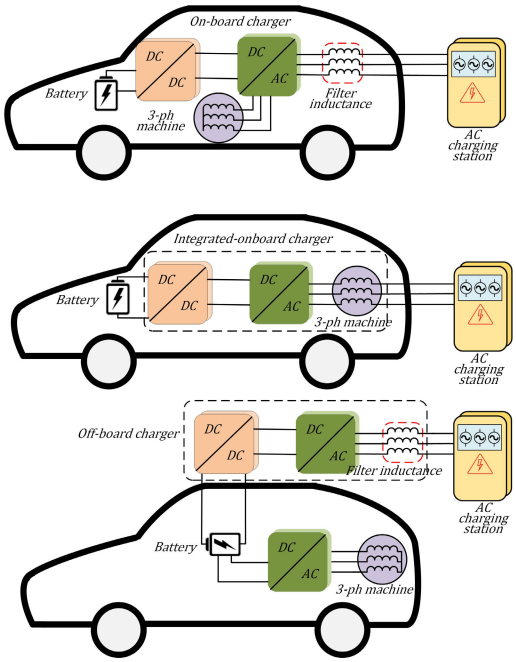

FIGURE 3. Classification of different types of EV chargers.

SynRMs have properties such as high reliability, torque, speed, and fault tolerance that are superior to those of other motors on the market [30], [34], [35], [36]. Based on reliability, fault tolerance, noise, and torque ripples, the SRM offers high performance over a wide range of speeds for EVs [37], [38], [39].

This review provides a systematic overview of EV charging technologies, covering both off-board and on-board charging schemes. The limitations of conventional off-board chargers are first examined to motivate the development of integrated on-board charging solutions. The core focus of this paper is on IOBCs, with a comprehensive review of machine-integrated and converter-integrated architectures. These IOBCs are further categorized into isolated and non-isolated topologies, with non-isolated configurations additionally classified as single-phase or three-phase grid supply. Each topology is analyzed in terms of operating principles, advantages, and inherent limitations. Control strategies for IOBCs are subsequently reviewed, with an emphasis on performance, control complexity, dynamic response, and reliability across charging, traction, and V2G operating modes. Although IOBCs offer advantages such as reduced cost, weight, and increased power density, their integration into the grid introduces several technical challenges. Accordingly, this review summarizes existing research addressing these challenges. It concludes by identifying future research directions in converter topology innovation, efficiency and reliability enhancement, wide-bandgap device adoption, thermal management, advanced control techniques, energy storage integration, and smart grid interaction.

II. SYSTEM-LEVEL CHALLENGES AND INFRASTRUCTURE CONSTRAINTS OF OFF-BOARD EV CHARGING STATIONS

As the automotive industry shifts from combustion-engine vehicles to EVs, the traditional refueling process must be replaced with charging solutions that are efficient, fast, widely accessible, cost-effective, and compact. Among the available charging methods, off-board charging stations stand out for their high power density, enabling fast charging and extended driving range—particularly for commercial EVs. However, these advantages come with several challenges, especially in terms of cost, land requirements, infrastructure availability, and grid-related constraints. The main limitations of off-board charging stations are outlined below.

A. IMPACT OF HIGH-POWER OFF-BOARD CHARGING ON GRID STABILITY

With the increase in EVs, the number of charging stations has risen significantly. On the one hand, having multiple charging stations at different locations is quite fruitful; on the other hand, it poses significant grid-stability issues due to the high power rating of these fast-charging stations. For example, the latest EVs equipped with fast charging can draw up to 350 kW from the grid at once [40]. Problems that arise due to the high penetration of EVs and PHEVs include, but are not limited to, voltage and current ripples, frequency dips, peak load demand, thermal and electrical overloading of distribution transformers, and the possibility of overstressing and destabilizing the grid when more loads are connected [41], [42], [43], [44].

Different authors used different techniques to analyze grid stability when EV chargers are connected to the grid. The authors in reference [45] used the IEEE 3-bus test system to observe the behavior of the grid with and without EV charging-station interaction and concluded that the grid becomes more unstable with the addition of charging stations. Similarly, the authors in [46] investigate the effect of EV penetration on the grid, with EVs serving as a source of grid power (i.e., V2G). The authors claim that using EVs as a grid energy source may improve the stability of the overall power system.

Researchers have proposed various solutions to mitigate grid stability issues arising from the integration of EV charging stations, including upgrading grid infrastructure, incorporating energy storage into charging stations, adopting Smart Grid and microgrid frameworks, integrating (RE) sources, employing power factor correction devices, and implementing voltage and frequency stabilization techniques [47], [48], [49]. Nonetheless, the implementation of these solutions must comply with the specific grid codes governing the connection of EV charging stations to the utility grid. One such code established by IEEE is IEEE-519, and to follow these codes, different power converter topologies are employed in the integration of EVs, such as bidirectional power flow, multi-port facilities, and the inclusion of PFC devices for better power regulation [50].

B. GRID UPGRADE REQUIREMENTS AND OPERATIONAL COST IMPLICATIONS

It will never be an easy task to upgrade the existing grid system to a new one compatible with the integration of the latest fast-charging technology, given the costs, volumes, availability, and complexity. For example, compared to upgrading a 50 kW charging station, a 350 kW fast charging station costs more when connected to a weak grid system [51]. Similarly, it is also not feasible to connect such high-power chargers directly to the HV or MV grid, especially in highway areas near villages where the grids are typically weak. Furthermore, due to the integration of high-power, fast DC charging stations into the existing grid, distribution lines, transformers, transmission lines, and equipment providing ancillary services need to be upgraded [52]. In addition, the heavy load put by these charging stations during peak hours of the day or month causes more power losses, transformer and feeder overload, and their aging [53], [54].

The power companies charge the utilities, i.e., charging stations, based on the peak power they draw in a month to recover their generation, transmission, and distribution costs. The demand charges in different countries vary; in the case of the US, it fluctuates between \$2/kW to \$90/kW [55]. A 300 kW charger used 24 hours a day, 365 days a year, will consume 2628 MWh of energy. The cost of electricity in California is roughly around \$16.67 cents/kWh [55] during normal hours and may be approximately \$30 to \$50 cents/kWh during peak hours. Furthermore, if the peak hour lasts about 7 hours, i.e., 12 PM to 7 PM or 8 AM to 3 PM during summer and winter, respectively, the cost of electricity for peak hours imposed by the charging station for the whole year is approximately \$229950/year at a rate of \$30 cents/kWh and \$338250/year at a rate of \$50 cents/kWh. However, with the use of an energy storage system (ESS) at the charging stations, this peak-hour cost will be significantly reduced by the ESS's services during the peak hour. Suppose that the ESS with its battery system operates at 90% efficiency and a 20 kW charger is required to recharge the ESS batteries from the grid. In this case, the grid experiences a peak load of 20 kW instead of 300 kW during peak hours. This reduction can lower peak-hour electricity costs by approximately \$15330/year at \$30 cents/kWh, and \$25550/year at \$50 cents/kWh, although additional costs for batteries and power converters will be incurred.

C. CHALLENGES IN RENEWABLE-ENERGY INTEGRATED OFF-BOARD CHARGING SYSTEMS

The electrification of the transportation sector, like many other sectors, is progressing to meet the demand to reduce greenhouse gas emissions [56]. However, this goal cannot be achieved without effective interaction among them and with the electrical grid. Integration of RE resources, such as wind and solar, with EVs and the grid is both challenging and essential, with the primary difficulties stemming from the intermittent nature of both RE generation and EV charging demand [57], [58]. The intermittent nature of these sources not only reduces the flexibility of the power system [59], but also leads to new challenges such as power quality [60], stability [61], and grid protection [62]. Voltage stability issues may arise due to slow dynamics or transient conditions in the power system [63]. Slow dynamic stability issues may arise due to gradual increases in load on the power system, whereas transient issues occur with the sudden addition or removal of load. Furthermore, induction generators draw significant reactive power as active power demand increases, which can degrade the grid's voltage profile and adversely affect power quality. On the other hand, the switching action of power electronic devices used in RE power generation, together with nonlinear devices, is a source of harmonics in the power system. These harmonics, if not properly mitigated, may cause power quality issues in the grid [64].

These challenges can be mitigated using various approaches, such as incorporating ESS [65], upgrading the grid infrastructure [66], implementing advanced forecasting techniques for wind and solar generation [67], [68], and applying demand response strategies [69], [70]. ESS for charging stations includes, but is not limited to, batteries, flywheels, hydrogen fuel systems, and hybrid configurations [13]. RE resources can be installed or deployed independently with the charging stations [71], [72], [73], or connected to the grid, mitigating grid stress by providing an additional energy source to EVs during peak hours [74].

With the penetration of more RE resources and EVs into the existing power system, there is a dire need for an independent, intelligent grid system that can operate with its own energy sources [75]. The microgrid facilitates EV charging by providing an additional energy source that allows charging at any time, thereby reducing the burden on the existing grid. In the research work of [76], the authors sought to convince the reader that integrating RE resources and EVs into the microgrid is crucial for energy management, cost reduction, and greenhouse gas emissions mitigation.

D. ROLE AND LIMITATIONS OF ENERGY STORAGE SYSTEMS IN OFF-BOARD CHARGING STATIONS

ESS plays a vital role in stabilizing power systems, particularly when incorporating intermittent RE resources and EVs. The ESS helps regulate not only the voltage and frequency to their nominal values when generation reduces, sudden faults occur, or heavy loads are connected to the system, but also enhances the system's flexibility. There are different types of ESS available on the market based on the energy storage method (chemical, electrochemical, mechanical, electrical, thermal, and thermochemical), such as battery energy storage systems (BESS), flywheels, supercapacitors, and pumped hydro storage [77], [78]. Various research articles have been published that compare the advantages and disadvantages of these energy sources based on charging capacity, discharge time, cost, applications, and availability [79], [80], [81].

Among ESS, BESS is the most attractive due to its simplicity, flexibility, efficiency, versatility, and modularity. There are different types of batteries available depending on the electrodes used in them, such as lead acid batteries, nickel–cadmium batteries, and Li-ion batteries [82]. Among them, Li-ion batteries proved to be more efficient in terms of life cycle, energy density, thermal stability, efficiency, and power density [83], [84]. Li-ion batteries are characterized based on the types of materials used for their positive and negative electrodes, such as lithium cobalt oxide (LCO), lithium manganese oxide (LMO), lithium nickel cobalt aluminum oxide (NCA), lithium nickel oxide (LNO), lithium iron phosphate (LFP), lithium titanium oxide (LTO), lithium nickel manganese cobalt oxide (NMC) [85].

BESS is now used in various applications, including grid storage systems, fast DC charging stations, EVs, critical loads, and industrial solutions [86]. The BESS supports charging stations by providing energy to charge vehicles and also provides ancillary services to the grid during peak hours; however, there are certain challenges associated with these services. The challenges include, but are not limited to, power-electronics limitations, energy-management systems, size, and cost.

Power electronic converters serve as an interface between the BESS and the DC or AC bus, controlling power flow, regulating bus voltage and current, and managing the charging of the BESS [87], [88], [89], [90], [91], [92]. There are different types of power converters capable of converting energy from DC-DC or AC-DC and featuring uni- or bidirectional power flow, such as Buck, Buck-Boost, Cuk, Sepic, Dual-Boost, Back-to-Back, Totem-Pole, and Vienna. These converters, which act as a medium between the BESS and the bus system, face limitations in various situations, including power density, current and voltage ripples, voltage stress, size, cost, complexity, and reliability [87], [93].

In charging stations, the energy flows between generating sources (Grid, PV, Wind), ESS (BESS, Flywheels, Super Capacitors), and load (EVs). Hence, an efficient and intelligent energy management system will need to monitor energy flow, regulate charging and discharging of ESS, and control power converters to optimize energy efficiency [87], [93], [94], [95].

Integrating high-power, fast DC charging stations with BESS poses challenges in sizing, lifespan, and control. To meet the charging demands of 150–350 kW per port, BESS often requires a large peak power capacity, resulting in high costs and underutilization during off-peak periods. Frequent high C-rate cycling accelerates battery degradation and increases replacement costs, while robust thermal management is essential for safety and performance. Effective real-time control is critical for coordinating BESS operation with charging demand, grid conditions, and state-of-charge targets; poor management can fail to mitigate voltage sags or demand spikes and may even exacerbate grid stress. In renewable-integrated systems, scheduling must balance variability smoothing with fast-charging support to preserve battery life.

TABLE 3. System-level cost comparison between conventional OBC and IOBCs.

Cost-determinants	Conventional OBC	IOBC
Dedicated converter hardware	High	Low
Magnetic Components	High	Low
Power semiconductor devices	High	Low
Packaging Volume and mass	High	Low
Thermal Management	Medium	High
Overall System-Level Cost Impact	High	Medium–Low

The system-level challenges associated with high-power off-board charging infrastructure strongly motivate the adoption of on-board charging solutions that can alleviate grid stress and reduce dependence on expensive charging infrastructure. However, the inclusion of standalone on-board chargers increases vehicle cost, volume, and mass, thereby adversely affecting overall power density and system efficiency. To highlight this trade-off, Table 3 presents a qualitative comparison of costs and hardware requirements between conventional on-board chargers and IOBC architectures, including component count, power-electronics utilization, and additional hardware requirements.

As a result, IOBCs have gained significant research attention, as they combine propulsion and charging functionalities within a unified hardware platform, enabling compact design, improved utilization of existing drivetrain components, and potential reductions in system-level cost.

III. INTEGRATED ON-BOARD CHARGER ARCHITECTURES FOR EVs

IOBCs have recently been developed to address the challenges of conventional on-board and off-board chargers, including their large size, high cost, and high power losses. Different techniques are used to better utilize electrical components during EV charging, each with its own merits and demerits. The classification is mainly based on device utilization during charging, such as traction motor (motor-integrated) and power converter (converter-integrated), and on the nature of the charger's supply voltage, i.e., single-phase and three-phase. Based on these classification criteria, different power circuit topologies are developed, where specific arrangements of power switches, diodes, capacitors, inductors, and other components enable controlled power transfer between the EV and the grid. Different converter topologies have their own pros and cons, which can be discussed in detail in the following section.

The IOBCs used components already available in the vehicle for charging. In the Motor Integrated Charger (MIC) topology, the traction motor is placed between the power

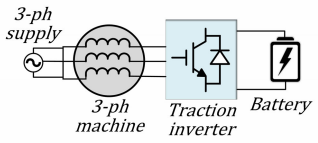

FIGURE 4. Single-stage MIC.

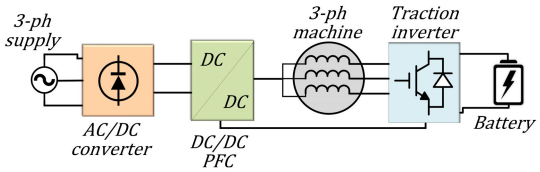

FIGURE 5. Dual-stage MIC.

converter and the charging station, and the motor's stator windings are used as filter inductors for the grid and the converter. The power from the charger is directly injected into the machine windings and subsequently transferred through the traction inverter to charge the EV battery. Similarly, during propulsion, the external relay or switch that connects the vehicle to the charger opens, and the battery begins to discharge as power flows in the reverse direction—from the battery to the electric motor. For this purpose, single-stage and dual-stage MIC topologies are used, as illustrated in Figs. 4 and 5, respectively. The difference between them is that, later, there is an additional front-end AC-DC converter and PFC circuit between the external grid and the rotating machine. Similarly, in the Converter Integrated Charger (CIC) topology, the power traction converter is placed between the external power supply and the electric motor, and hence the integrated converter acts as a medium for power flow among the motor, ESS, and external power supply. For this type of charger topology, an external filter inductance is needed to suppress power harmonics, which, in the previous case, was provided by the motor winding inductance. The circuit diagram of single- and dual-stage CIC is shown in Figs. 6 and 7 respectively.

Furthermore, IOBCs are classified according to their topologies, which can be either isolated or non-isolated. For achieving an isolated configuration, different techniques are used, such as the utilization of a bidirectional DC-DC converter with a solid state transformer [96], [97], inclusion of machine rotor and stator windings for isolation [98], [99], or using a low frequency line transformer [100]. Similarly, the non-isolated chargers are categorized into single-phase and multi-phase machine drives. The non-isolated schemes use motor windings as filter,inductors, and the inverter legs are directly connected to the phases of the machine windings; hence, the inverter operates as an active front-end rectifier during charging. The detailed classification of isolated and non-isolated integrated chargers is described in the following subsections.

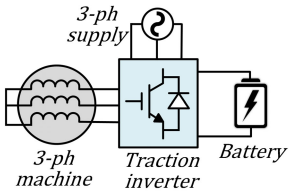

FIGURE 6. Single-stage CIC.

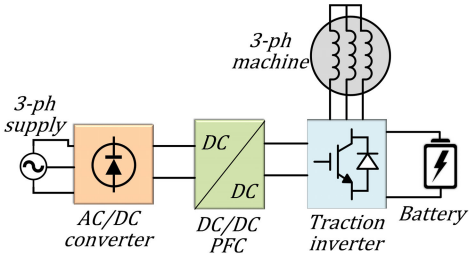

FIGURE 7. Dual-stage CIC.

A. ISOLATED IOBCs

The idea of isolated IOBCs was first presented by F. Lacressonniere and B. Cassoret in their work on the control of the power converter of an industrial truck, both during charging and speed-control modes [97]. The first case was tested on a pallet truck operated by a 1.5 kW DC motor, and the second analysis was carried out on a forklift based on a 6 kW Wound Rotor Induction Machine (WRIM) as depicted in Figs. 8 and 9 respectively. For the first one, to achieve galvanic isolation, a bidirectional DC-DC Cuk converter with PFC is used. This converter works in both modes: controlling the traction motor during propulsion and charging the battery while the vehicle is connected to the external grid by acting as a rectifier. In the second case, the WRIM windings provide isolation, thereby mitigating the impact of the grid on the vehicle and vice versa. In particular, the external three-phase voltage source is directly connected to the rotor windings, and a three-leg bidirectional power converter, which is used to rectify the AC voltage from the stator winding, is connected to the storage battery whose nominal voltage is 48 V. Switching between different modes is done with the help of contactors which connect the rotor windings to the external source during charging mode and short circuit them during traction mode as shown in Fig. 9. The major drawbacks of the proposed topology are the high magnetizing current requirement and the additional cost imposed by the wound rotor and contactor implementation.

In [101], a multi-port isolated DC–DC converter is proposed for an IOBC, where the on-board charger and auxiliary power module are combined into a single converter, as shown in Fig. 10. The converter enables simultaneous charging of the HV and LV batteries from the grid, as well as charging the LV battery from the HV battery, without the use of contactors. Galvanic isolation between the grid,

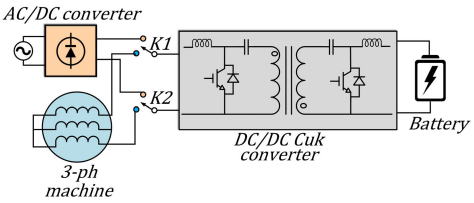

FIGURE 8. Converter used as a battery charger and a motor speed controller in an Industrial Truck [97].

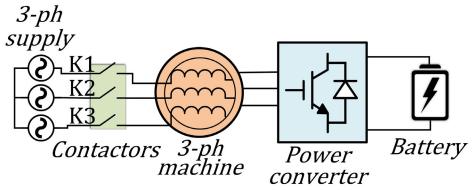

FIGURE 9. Converter used as a battery charger and a motor speed controller in a Forklift truck [97].

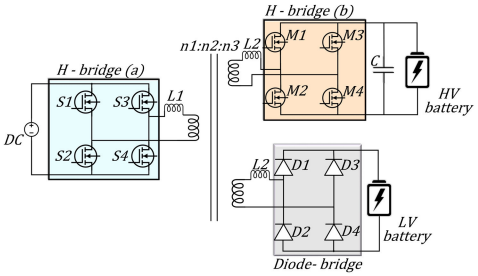

FIGURE 10. Integrated on-board charger with multiport DC-DC converter enabling independent HV and LV battery charging [101].

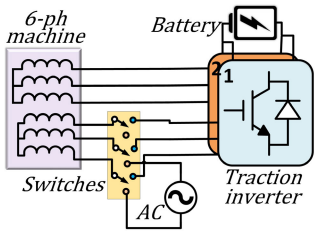

FIGURE 11. Single-phase galvanically isolated integrated on-board charger embedded in a 6-phase traction motor e-drive [102].

the HV battery, and the LV battery is provided by a single three-winding high-frequency transformer with a turn ratio of $n_1 : n_2 : n_3$. Port 1 is connected to the grid through an active front-end rectifier with PFC, while ports 2 and 3 interface with the HV and LV batteries, respectively. Ports 1 and 2 employ H-bridge converters and support bidirectional power flow, whereas port 3 is connected to the LV battery through a unidirectional diode rectifier. The topology utilizes a reduced switch count (eight switches and four diodes), achieves ZVS operation, and delivers up to 3 kW to the HV battery (250–450 V) and 500 W to the LV battery (8–16 V), with a reported peak efficiency of 94%. However, the analytical model neglects the transformer magnetizing inductance, operates at a relatively high switching frequency of 100 kHz, and achieves a modest peak efficiency compared to state-of-the-art EV on-board charging solutions.

Researchers have also investigated the use of electric motor windings to provide galvanic isolation for on-board chargers in isolated EVs. Two main approaches have been reported: using both stator and rotor windings, or employing stator windings alone in multiphase machines [102]. In [102], a single-phase grid source is integrated with a six-phase traction drive and a multiphase PMSM to realize an isolated on-board charger, as illustrated in Fig. 11. The proposed system employs two identical three-phase two-level inverters, each connected to a symmetrical three-phase stator winding set during traction operation. In charging mode, one inverter is disconnected, and the single-phase grid is directly connected to selected phases of the remaining stator winding set, such that the two symmetric stator windings function as an isolation transformer. The charger supports bidirectional power flow (G2V and V2G) with a maximum charging power of 6 kW under constant-current or constant-voltage operation. Despite achieving isolation via machine windings, the topology requires hardware reconfiguration between traction and charging modes. It relies on contactor switches, resulting in additional losses, increased complexity, and potential reliability concerns.

To achieve isolation, some researchers used coupled magnetic-based devices (CMD) between the utility grid and the on-board charger, as demonstrated in Fig. 12 [103]. This CMD acts as a boost inductor during charging mode and as an isolated transformer during AC-DC conversion, depending on the boost converter's phase angle. As shown in Fig. 12, the charger's topology consisted of an AC-AC matrix converter, CMD, boost converter, and a dual three-phase inverter. The authors claim that using four-leg CMD, which utilizes high inductance and reduces switching frequency, can increase efficiency and power density by up to 1.5% and 12%, respectively. This topology suffers from reduced AC charging efficiency due to elevated conduction and switching losses caused by single-phase current fluctuations—in addition, substantial core losses—optimized for traction operation further limit charging performance.

The authors in [104] used an IPM-based synchronous machine for the EV, equipped with an isolated on-board charger, as shown in Fig. 13. The proposed system comprises nine slots and an eight-pole combination with a non-overlapped fractional-slot concentrated winding. The nine slots with nine-phase windings are arranged so they can be connected to the six terminals of the six-phase inverter. In propulsion mode, switches S1, S2, and S3 are closed, and different sets of six front phases of the motor windings are used by selecting different positions of the "K" switches to transfer power from the battery source to the stator windings of the IPM machine. In charging mode, the switches S1, S2,

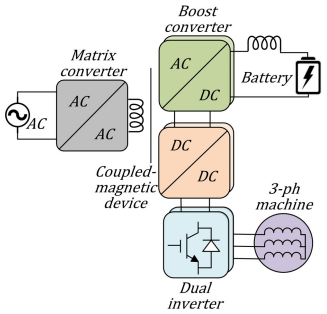

FIGURE 12. Four-leg CMD-based single-phase integrated isolated on-board battery charger and boost converter for EVs [103].

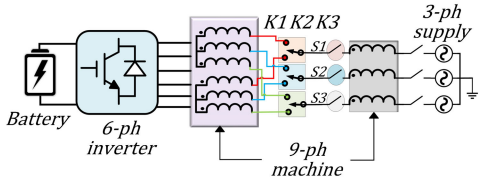

FIGURE 13. Nine-phase six-leg IPM based isolated integrated on-board charger [104].

and S3 are opened; the three-phase power from the grid is connected to the three-phase winding of the machine, and the remaining six phases of the machine act as a rotating transformer with the first three-phase winding acting as the primary and the remaining six phases as a secondary winding. Due to the rotational effect of the machine, an additional clutch will need to separate the machine from the mechanical system during charging. A key limitation of this method is the increased system complexity, along with undesired motor rotation during charging operation.

B. NON-ISOLATED IOBCs

Non-isolated IOBCs are chargers that do not provide galvanic isolation, which is necessary for the safe operation of the EV and protection of users, as they are susceptible to leakage currents. In such a charger, the grid is either directly connected to the phase winding of the machine (machine integrated) and the machine windings act as a filter inductor for the grid, or it is connected to the traction converter (converter integrated) first, then the power is transferred to the battery for charging purposes.

Non-isolated IOBCs can be further classified into three categories based on the type of grid power supply and the method of power transfer: single-phase chargers, three-phase chargers, and wireless chargers. Among them, the first is the slow-charging technology, which is readily accessible, while the remaining two have fast-charging capability but are not readily accessible everywhere.

1) SINGLE-PHASE EV CHARGER

The first and most widely used charging technology in the field of EV is the single-phase EV charger, which is easily

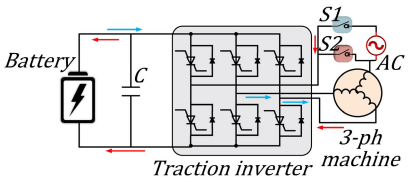

FIGURE 14. An SCR-based inverter with an integral battery charger [108].

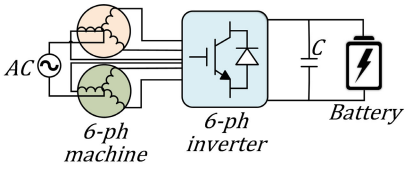

FIGURE 15. Single-phase IOBC for EVs based on multiphase machines [107].

available at the domestic level. However, the slow charging nature of these chargers imposes a significant limitation on their use at scale. In addition, the pulsating current from these chargers significantly shortens the lifespan of the storage batteries used in EVs in long-term scenarios [105], [106]. These single-phase EV chargers are suitable for charging both single-phase machine-associated EVs or multi-phase machine EVs. A detailed discussion of all these types of chargers and related machines will be presented in the following section.

The first single-phase EV charger was proposed in 1985 by Thimmesch [107], employing an SCR-based converter and an isolated transformer, as shown in Fig. 14. The system enabled charging of a 25 kWh battery within 8 h. The topology comprised an SCR-based three-phase inverter with freewheeling diodes, a battery pack, and a three-phase AC motor. In charging mode, switch S1 was closed, and S2 was open, allowing power transfer from the single-phase AC grid to the battery via AC–DC conversion, while the motor windings served as the grid-side filter inductance. In traction mode, S1 was opened, and S2 closed, enabling power flow from the battery to the motor via DC–AC conversion. The reported performance included an efficiency of 86% and a power factor of 0.95 at 3.6 kW and 220 V AC. However, the topology requires a fourth inverter leg to provide a neutral current return, which must be rated at three times the current of the other legs, representing a major drawback.

A similar approach was investigated in [108], where the authors used different multi-phase machines, such as a nine-phase, a six-phase, and a five-phase machine, with a single-phase AC source, as shown in Fig. 15. Since all multi-phase machines employ a similar grid-connection topology—namely, connecting the machine neutral point to the AC source—this study focuses exclusively on the six-phase machine. The AC source from the grid is directly connected to the neutral point of the multi-phase machine, and hence the machine winding acts as a filter for the grid, and

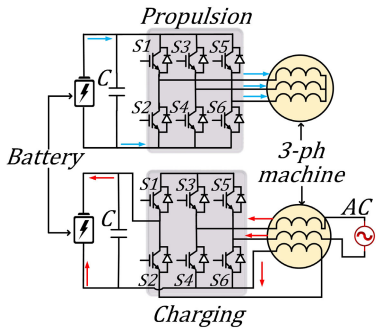

FIGURE 16. Single-phase buck-boost integrated charger topology utilizing a three-phase PMSM [110].

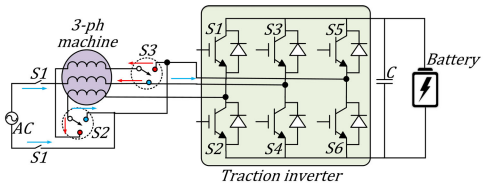

FIGURE 17. Induction motor-based single-phase integrated battery charger with active power decoupling [109].

there is no need for hardware reconfiguration during charging and propulsion mode, as shown in Fig. 15. Furthermore, the proposed model produces zero charging torque and can transfer power between V2G and G2V with a unity power factor.

A single-phase isolated on-board battery charger with zero-torque operation and buck–boost capability is presented in [109] and shown in Fig. 16. It uses a three-phase PMSM, a two-level inverter with winding reconfiguration, relays, and filter capacitors to enable battery charging from a single-phase supply. At the same time, in traction mode, power flows from the battery to the motor through the inverter. In Fig. 16, the current path during traction mode is shown by blue arrow lines, and red arrows are used to depict the charging process. The motor windings also act as a ripple filter for the grid, and the charger operates in boost or buck mode depending on whether the input voltage is below or above the battery voltage.

Another single-phase integrated on-board charger based on model predictive control with active power decoupling is presented in [110] and presented in Fig. 17. During charging, switch S1 is closed while S2 and S3 are set in the blue position, configuring two stator windings of the three-phase induction motor in parallel to share current, suppress twice-line-frequency DC-link ripple, and ensure zero torque operation through balanced currents. In traction mode, S1 is opened, and S2 and S3 are switched to the red position, forming a star-connected motor configuration, while the inverter operates at a reduced switching frequency to minimize losses and improve efficiency. However, the main limitation of this topology is the increased hardware

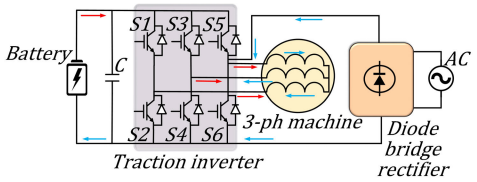

FIGURE 18. Single-phase boost-type integrated on-board charger based on PMSM winding inductance [111].

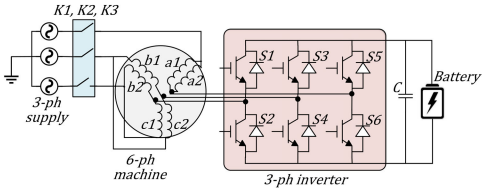

FIGURE 19. Integrated on-board battery charger using asymmetrical six-phase machine stator windings and a three-leg traction inverter [112].

complexity and cost due to the high number of switches required.

Chuan Shi, Yichao Tang, and Alireza Khaligh proposed a single-phase IOBC that utilizes the EV propulsion system with a PMSM [111], as illustrated in Fig. 18. The charger achieves higher efficiency than conventional solutions due to its simple structure, unity power factor operation, ripple-free charging current without bulky passive components, and zero torque production during charging. In charging mode (blue current paths in Fig. 18), a diode-bridge rectifier performs AC–DC conversion, while two machine windings operate as an interleaved boost converter with the traction inverter disabled; in traction mode (red current paths in Fig. 18), the rectifier is bypassed, and the battery supplies the star-connected motor through the inverter. To reduce current ripple and improve harmonic performance, the topology operates in continuous conduction mode. However, incorporating additional components increases control complexity and conduction losses.

2) THREE-PHASE EV CHARGER

Fast and high-power charging can be achieved using either a three-phase AC power supply or by external fast DC charging stations. Until now, many different charging topologies with three-phase power supply have been described in the literature.

A three-phase integrated charging topology employing a split-phase asymmetrical motor for both charging and traction is presented in [112] and illustrated in Fig. 19. To reduce cost and volume, the three-phase inverter legs are reconfigured for dual-mode operation, enabling zero-torque charging, fast charging capability, and grid-support functions such as unity power factor and V2G operation. Mode transition is achieved using single-pole double-throw contactors to reconfigure the machine windings, resulting in different parallel winding combinations and inherently unbalanced phase inductances.

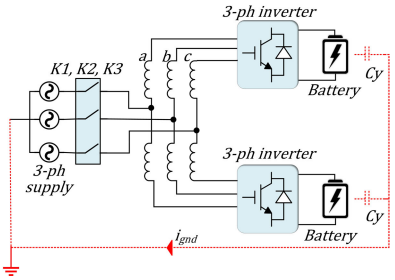

FIGURE 20. Integrated three-phase on-board charger based on dual-inverter drivetrain and split-phase electric machine [113].

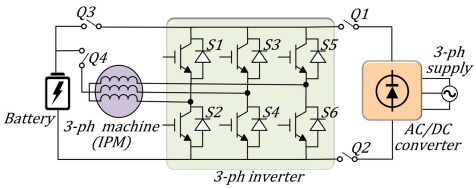

FIGURE 21. Integrated on-board charger based on three-phase IPMSM and reconfigured propulsion inverter [26].

During charging, contactors K1–K3 are closed to transfer power from the AC supply to the battery via the machine windings, whereas in propulsion mode, the contactors are opened and power flows from the battery to the split-phase motor.

Another three-phase integrated charger based on a split-phase motor and a dual-inverter architecture is presented in [113] and illustrated in Fig. 20. The topology requires minimal additional components by exploiting a split-phase machine. It supports four operating modes—charging, driving, zero-sequence current generation, and grid common-mode current control—through independent subsystems with six degrees of freedom. The charging system employs dual inverters supplied by separate battery packs, preventing zero-sequence circulating currents while offering improved fault tolerance, good harmonic performance, zero-torque charging, and wide-speed-range operation. During charging, the three-phase grid is directly connected to the machine split-phase point, the vehicle body is grounded for safety, and the parasitic capacitance (Cy) between the battery pack and the vehicle body provides a path for the common-mode current, which is continuously monitored and minimized to avoid the protective device tripping. A key limitation of this topology is the specialized machine design for split-phase windings, and the dual-inverter approach further increases cost and compromises power density.

The authors in [26] investigated the safe charging of an IOBC using an IPM motor, analyzing the charging torque and current ripples. The system, shown in Fig. 21, employs a rectifier, an inverter, motor windings, a storage battery, and four reconfigurable switches (Q1–Q4) to enable transition between traction and motoring modes. Charging mode is initiated by closing all switches except Q3,

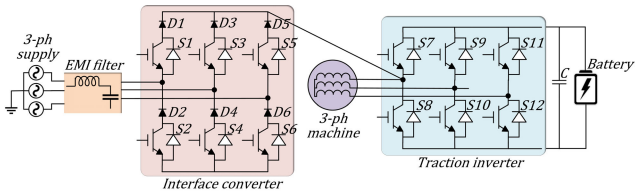

FIGURE 22. Three-phase on-board charger integrated with the propulsion system using the PMSM as a coupled DC inductor [18].

allowing AC power to flow to the battery, while traction mode is achieved by reversing the switch positions. The total torque during charging is the sum of the electromagnetic torque and the reluctance torque, with the electromagnetic torque derived from the motor's magnetic co-energy. The authors also reported that current ripples can be minimized using smoothing reactors and high-frequency operation, and that the front-end rectifier supports unity power factor operation with single- or three-phase AC supply. The main limitation of this topology is the use of additional switches for hardware reconfiguration between charging and traction modes, which increases system complexity and cost.

A three-phase integrated charger for plug-in EVs is presented in [18] and illustrated in Fig. 22. The PMSM windings act as coupled inductances between the source- and battery-side converters, enabling high-power-factor operation and voltage- and current-controlled charging without reconfiguring the windings or adjusting components. During charging, switches S7 and S8 are disabled, allowing current to flow through the remaining inverter arms, while the interface converter adapts operation between charging and propulsion modes. The authors report high power density (3.3 kW), low THD (4.77%), zero charging torque, and efficiency up to 92.6%. However, the use of additional switches, complex control strategies, and higher cost can limit the topology's effectiveness. A similar integrated charger discussed in [111] omits the interface converter and front-end diodes, operates from a single-phase AC source, and achieves slightly higher efficiency (up to 93.1%).

An integrated battery charger that uses a dual-inverter and an induction motor as the propulsion system is presented in [114] and illustrated in Fig. 23. A three-phase supply with a rectifier provides the front-end DC source, and no hardware reconfiguration is needed during charging. The charger reduces inrush and DC short-circuit currents, while its 2-level three-phase design lowers input voltage THD. Operating in both buck and boost modes, the machine windings serve as storage inductors, minimizing weight, volume, and cost. The control architecture synchronizes the rectifier and dual inverters to maintain proper voltage between the storage elements during all operating modes. However, the main limitation of this topology is the need for an additional current-source converter during charging, which increases the total system cost.

A three-phase fast integrated charger based on segmented PMSM windings is presented in [115] and illustrated in

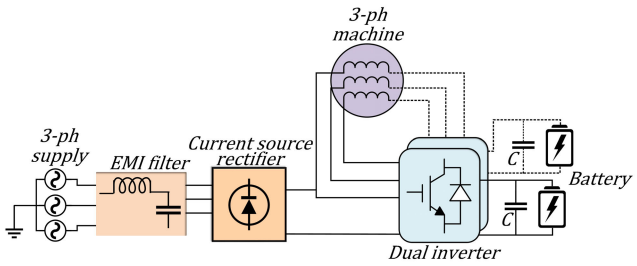

FIGURE 23. Three-phase integrated charger using a dual-inverter open-winding induction motor configuration [114].

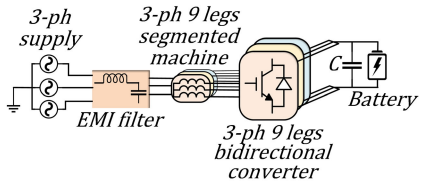

FIGURE 24. Integrated on-board charger using segmented windings of an IPM motor with three phases and nine windings [115].

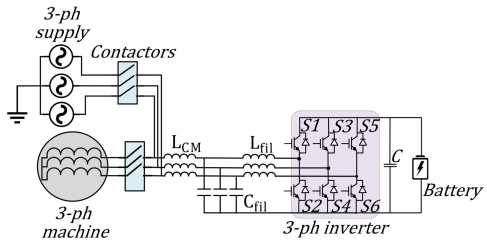

FIGURE 25. Bidirectional EV charger employing traction inverter with LC and common-mode filtering for high efficiency [116].

Fig. 24. The topology supports both single- and three-phase grid supplies, with the battery directly connected to the neutral point of a nine-winding PMSM during charging and propulsion. Segmented windings enable improved controllability, low-voltage operation using lower-rated switches, and zero torque production during charging due to magnetic field cancellation. The 18-switch traction converter operates as a boost rectifier to achieve a unity power factor, while a nine-leg bidirectional boost converter transfers grid power to the battery. However, the high component count significantly increases circuit complexity and cost.

A bidirectional, non-isolated, on-board integrated charger is presented in [116] and illustrated in Fig. 25, with a primary focus on reducing common-mode voltages and currents to improve system reliability and motor bearing lifetime. An LC filter and an additional leakage-current suppression inductor are employed to mitigate common-mode effects, while a variable-frequency soft-switching technique reduces the size of the magnetic component and enhances efficiency. The authors report a reduction of up to 90% in common-mode voltage and current, and an efficiency of 98–99% at a rated power of 11 kW. However, additional inductive and capacitive components increase cost and volume and can negatively impact overall efficiency.

To summarize the various aspects of the previously discussed topologies, a holistic comparative evaluation is conducted using multiple criteria critical to IOBC applications. These criteria include the nature of the supply, machine type, hardware reconfiguration requirements, traction power availability during charging, bidirectional power flow capability, current ripple mitigation, switching frequency, overall efficiency, zero charging torque operation, and galvanic isolation. Rather than relying on a single performance metric, the relative promise of each topology is assessed based on its ability to satisfy a greater number of these criteria simultaneously while maintaining practical feasibility. A comprehensive comparison of the reviewed topologies is presented in Table 4. It is worth noting that the values reported in Table 4 are extracted from studies conducted under different power ratings and operating conditions; therefore, the comparison is intended to highlight topology-intrinsic capabilities, design trade-offs, and performance trends rather than to provide a normalized quantitative benchmark.

IV. CONTROL TECHNIQUES FOR AN IOBC

This section systematically reviews the control strategies employed in IOBCs, with particular emphasis on their performance, computational burden, dynamic response, robustness, and practical feasibility for automotive applications. Due to the multifunctional nature of IOBCs, the control objectives differ fundamentally between G2V charging and V2G operation, necessitating distinct control architectures and design considerations.

In charging mode, primary control objectives include accurate current regulation, constant-current–constant-voltage (CC–CV) battery charging, grid power-factor control, compliance with harmonic standards, and strict suppression of electromagnetic torque to ensure torque-free and mechanically safe charging operation. These objectives are typically achieved through coordinated control of the traction inverter and charging power converter, using mode-dependent sensing and feedback structures. Accordingly, a dedicated subsection discusses widely adopted G2V control techniques—including PI/PR-based controllers, model predictive control (MPC), fuzzy logic control, and sliding-mode control, highlighting their advantages and limitations in terms of implementation complexity and real-time feasibility.

In V2G mode, the IOBC operates as a grid-connected inverter, introducing additional control challenges beyond those of unidirectional charging. These include grid synchronization, active and reactive power regulation, harmonic mitigation, islanding detection, and safe mode transition between charging, discharging, and traction operation. Therefore, a separate subsection focuses on V2G-specific control strategies and protection requirements, emphasizing their interaction with grid codes and automotive safety constraints.

TABLE 4. Summary of various IOBC topologies used for EV charging.

Ref.	Nature of supply	Machine type	Hardware reconfiguration	Traction power	Bidirectional power flow	Current ripple mitigation	Switching frequency	Efficiency	Zero charging torque	Galvanic isolation
[97]	Single-phase	DC Machine	No	1.5 kW	No	–	20 kHz	90%	Yes	Yes
[101]	Single-phase	–	Yes	3.5 kW	Yes	–	100 kHz	94%	Yes	Yes
[102]	Single-phase	Six-phase PMSM	Yes	96 kW	Yes	Yes	0.24 kHz	93%	Yes	Yes
[103]	Three-phase	Nine-phase IPMSM	Yes	40 kW	No	No	5 kHz	87%	No	Yes
[104]	Three-phase	Split-phase PMSM	Yes	25 kW	No	No	12 kHz	–	No	Yes
[108]	Single-phase	Asym. Nine, Six-phase and Sym. Six, Five-phase IM	No	1.1–2.2 kW	Yes	Yes	20 kHz	86%	Yes	No
[109]	Single-phase	Three-phase PMSM	Yes	1.3 kW	No	–	50 kHz	–	Yes	No
[110]	Single-phase	Three-phase IM	Yes	3.7 kW	Yes	Yes	Variable	–	Yes	No
[111]	Single-phase	Three-phase PMSM	No	3 kW	No	Yes	15 kHz	93.1%	Yes	No
[112]	Three-phase	Asym. Six-phase IM	Yes	10 kW	Yes	Yes	5 kHz	91%	Yes	No
[113]	Three-phase	Split-phase PMSM	No	7.2 kW	Yes	Yes	10 kHz	–	Yes	No
[26]	Three-phase	IPM	Yes	4 kW	No	Yes	20 kHz	90–95%	No	No
[116]	Three-phase	Three-phase PMSM	Yes	11 kW	Yes	Yes	Variable	98.4%	No	No
[117]	Three-phase	Three-phase PMSM	No	1 kW	Yes	Yes	Variable	–	Yes	No
[118]	Single-phase	Three-phase PMSM	Yes	3.3 kW	Yes	Yes	Variable	–	Yes	No
[119]	Single-phase	Six-phase PMSM	Yes	2 kW	Yes	No	2.2 kHz	–	Yes	No
[120]	DC	Three-phase PMSM	No	9 kW	Yes	No	20 kHz	–	Yes	No
[121]	DC	Three-phase PMSM	Yes	2.3 kW	Yes	Yes	10 kHz	–	Yes	No
[122]	DC	Three-phase PMSM	No	11 kW	No	Yes	7.5 kHz	–	No	No
[123]	DC	PMSM/ Induction machine	Yes	4 kW	Yes	No	20 kHz	–	No	No
[124]	DC	Three-phase PMSM	No	3 kW	No	Yes	10 kHz	95.9%	Yes	No

A. CHARGING MODE CONTROL SCHEMES

In charging mode, the EV is connected to an external power supply, which can be a single-phase or three-phase charging station or a DC charging station. In this case, machine windings act as filter inductance and energy-storage elements for an AC grid and for buck-boost operation. In this mode,

the charging station gets the charging current reference from the battery management system (BMS) of the vehicle, and the battery is charged in most cases by the CC-CV profile. The controller ensures that during charging, the charging current and voltage are within their limits to avoid overcharging and undercharging. Further, it is responsible for managing the thermal system and the state of charge (SOC) of the battery to prevent thermal runaway and extend battery life. In an integrated battery charger, a small charging torque is generated during the charging mode due to the use of the machine's windings for energy transfer. The controller also prevents rotor movement during charging to ensure the vehicle's safety. The power flow between the vehicle and the grid in V2G and G2V must be regulated by the control scheme when the vehicle is connected to the grid. Different types of linear and non-linear controllers, along with their working principles, are discussed in detail in the section below.

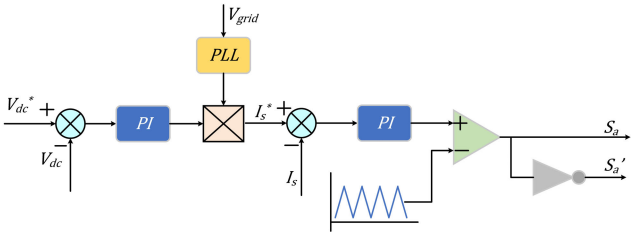

FIGURE 26. PI control strategy for EV charger.

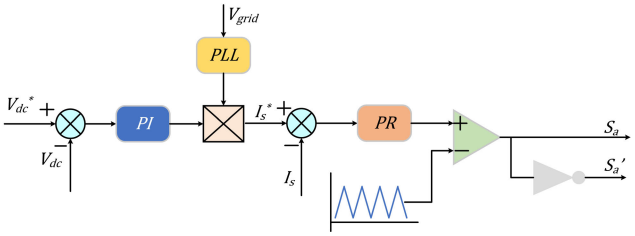

FIGURE 27. PR controller technique for EV charging.

1) PROPORTIONAL INTEGRAL CONTROLLER

The Proportional Integral (PI) controller is typically used in an EV charger during charging mode to control the voltage, current, and power to their reference values. The PI controller can improve system stability and prevent significant disturbances during operation [125]. In an IOBC, the DC-link voltage and the grid current are controlled by an AC-DC converter using two PI controllers as described in [126] and [127]. In [128], the authors implemented a dual-loop control strategy to regulate the charging current and achieve PFC. They used two PI controllers: one in the outer loop (for PFC) and the other in the inner loop (for charging current control). The dual-loop control technique, where the outer loop manages the DC-link voltage and performs PFC using a PI controller, is detailed in [117]. The error between the actual and reference signals is used to generate the control signal. This control signal is then used to control the power converter by generating an appropriate switching signal using any PWM techniques to control the converter's switches, as shown in Fig. 26. To synchronize all variables with the grid's phase voltage and current, a Phase-Locked Loop (PLL) is used to obtain the angular position ϑ of the grid. This angular position, ϑ, is used during the transformation of the reference frame, namely the Park transformation and its inverse, for the phase voltage and currents. However, when the load is significant and the system parameters change more frequently, the PI control technique shows performance degradation [129].

The transfer function of the PI controller is described by

$$G_c(s) = K_p + \frac{K_i}{s} \tag{1}$$

where K_p and K_i are the proportional and integral gains of the controller, respectively.

2) PROPORTIONAL RESONANT CONTROLLER

The Proportional Resonant (PR) controller is used to control the AC charging current during charging mode and extends the PI controller, with the integral part implemented as a generalized integrator in the stationary reference frame. Unlike the PI controller, the PR controller works in the frequency domain, which means it can track a sinusoidal reference signal having a varying frequency with zero error and without the need for any complex coordinate transformation, as shown in Fig. 27. To prevent torque generation during charging mode in an IOBC, identical currents in both magnitude and phase must flow through the motor windings. To achieve this, three different PR controllers are used in the inner loop of the charger, and the outer loop is responsible for maintaining the DC-link voltage and the PFC [117]. Similarly, to control the charging current in the moving reference frame, a PR controller with a gain of 100 dB at the grid frequency is used in [112] to achieve zero steady-state error. The values of K_i and ω are determined from the placement of poles and zeros in the transfer function of the system. A set of PR controllers has been used in [22] to regularize the charging current at the fundamental frequency and to mitigate the major harmonic contents such as 3^{rd}, 5^{th}, 7^{th}, and 9^{th}. The transfer function of the PR controller is expressed as

$$G_c(s) = K_p + K_r \frac{2\omega_c s}{s^2 + \omega_0^2} \tag{2}$$

where K_p and K_r are the proportional and resonant gain, ω_0 is the resonant frequency, and ω_c is the cut-off frequency that determines the bandwidth around the resonant frequency.

3) MODEL PREDICTIVE CONTROL

The fundamental principle of Model Predictive Control (MPC) is to forecast the behavior of a system based on its current state and input signals, using a mathematical model of the system under control. The basic circuit diagram of the

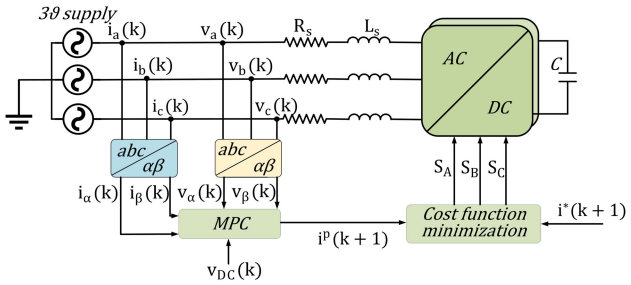

FIGURE 28. MPC-based controller algorithm for EV charging and traction application.

MPC used to charge the battery from three-phase AC sources is depicted in Fig. 28. The controller then determines the best course of action to satisfy the cost function using this forecast. Different performance goals, such as reducing the switching frequency, limiting current ripple, minimizing harmonic distortion, or optimizing efficiency, can be considered when designing the cost function.

The MPC is used in an IOBC to control the charging current, reduce harmonics, maintain the DC-link voltage, achieve unity power factor operation, and provide active power decoupling. In [110], the authors utilized the MPC to control the grid side current and the charging current, that is, the current flows through the windings of the induction motor. The controller used a reduced switching frequency to minimize switching losses, and due to its decoupled control, the harmonics in the battery current are greatly reduced. The MPC will start operating only when the difference between the reference and actual currents exceeds a predetermined threshold, and the voltage vector that minimizes switching loss is selected. MPC is used for power-factor correction, reference-current tracking, and SOC management of batteries in [130]. Reference current tracking is achieved by minimizing the cost function, which is the difference between the measured and predicted inductor currents. As the inductor current is locked to the input voltage by a PLL, accurate reference tracking ensures unity power factor operation. For SOC control, the MPC continuously monitors the charging level of each battery, and if the charging level of any battery falls below a predefined threshold, the control system activates to charge the battery until its charging level reaches the desired reference value.

MPC is used for charging current and voltage regulation to enable both buck and boost operation [118]. A linear outer control loop generates the grid current or voltage reference $i^*(k)$, which is extrapolated to the $(k+1)^{th}$ sampling instant and used by the MPC for prediction. Based on a discrete-time system model, the MPC predicts the future grid current and formulates a cost function that minimizes the error between the predicted current and the reference at the $(k+1)^{th}$ sampling instant by selecting the optimal charging switching state. Depending on the input voltage level relative to the DC-link or battery voltage, the controller seamlessly transitions between buck and boost modes. This smooth mode transition improves performance during grid voltage zero-crossing instants and ensures accurate current tracking with minimal ripple. In addition, MPC effectively regulates active and reactive power exchanged with the grid and suppresses high-frequency components, as reported in [131].

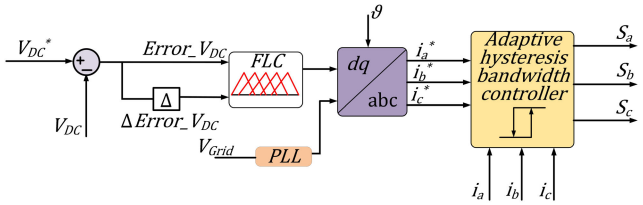

FIGURE 29. Fuzzy logic controller-based charging scheme.

4) FUZZY LOGIC CONTROLLER

A fuzzy logic controller (FLC) is a good choice for controlling non-linear systems without requiring a mathematical model and for handling uncertainty. Its working principle is mainly based on experience rather than complex equations. It can be combined with PI, PID, and hysteresis bandwidth controller to get the best of both, having a smooth response and easy tuning. Fig. 29 presents the implementation of the fuzzy logic controller alongside the adaptive hysteresis band controller. Typically, it gets two inputs, i.e., error and change of error, and consists of three main steps, including fuzzification, a base rule unit, and defuzzification [132], [133], [134].

A fuzzy controller in an IOBC typically uses inputs such as battery current error, voltage deviation, or torque ripple amplitude, and applies a rule base derived from expert knowledge to generate appropriate control actions, including switch commands, duty cycles, or modulation indices. The FLC processes these inputs through fuzzification, applies fuzzy inference rules, and outputs a control signal via defuzzification. In [135], the authors used FLC in conjunction with an adaptive hysteresis bandwidth controller to control the DC-link voltage of the rectifier up to the level required by the charging scheme of the battery, which is CC-CV. The FLC receives DC-link voltage error and change in voltage error as inputs and gives a discrete d-axis current variation as a reference d-axis current. A similar approach is presented in [136], where an FLC is employed to tune the gains of two identical PI controllers adaptively. This adaptation is necessary due to variations in the DC-link voltage during operation. To achieve this, the FLC uses the DC voltage error and its rate of change as inputs, enabling real-time adjustment of the PI parameters to improve dynamic performance and voltage regulation.

5) SLIDING MODE CONTROL

Sliding mode control (SMC) offers a simple and robust solution for non-linear systems having uncertainties, parameter

TABLE 5. Comparative analysis of different control strategies for charging mode of EVs.

Characteristic	PI Control	PR Control	MPC	Fuzzy Logic	Sliding Mode
Design Complexity	Low	Medium	High	Medium-High	Medium
Tuning Effort	Moderate	Challenging	High	High	Moderate
Dynamic Response	Slow	Fast (AC)	Very Fast	Medium	Very Fast
Steady-State Error	Present	Zero (at ω_0)	Very Small	Small	Zero
Robustness	Poor	Moderate	Good	Excellent	Excellent
Nonlinear Handling	Poor	Poor	Good	Excellent	Excellent
Computational Load	Low	Medium	Very High	High	Medium
Harmonic Rejection	Poor	Excellent (at ω_0)	Good	Good	Excellent
Parameter Sensitivity	High	Medium	Medium	Very Low	Very Low
Implementation	Simple	Moderate	Complex	Complex	Moderate
Mathematical Modeling	Required	Required	Required	Not Required	Required
Best Application	DC systems	AC systems with fixed frequency	Fast dynamics systems	Complex nonlinear systems	Robust control systems

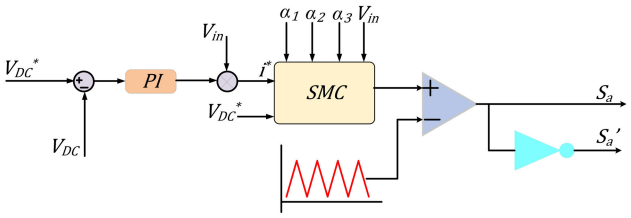

FIGURE 30. Charging technique based on SMC controller.

variations, and external disturbances. Its basic principle is to drive the system state onto a predefined surface, called the sliding surface, and force it to slide along this surface towards the desired operating point. The basic scheme of the SMC is shown in Fig. 30. SMC exhibits a fast convergence rate and good tracking performance, making it suitable for systems with time-varying and dynamic behavior. However, despite the advantages mentioned above, it also suffers from issues such as high chattering in the control input and a long time for the actual signals to converge towards the reference signals.

A sliding surface S(t) that drives the system towards convergence for stability is given by:

$$S(t) = \frac{d}{dt}e(t) + \lambda e(t) \tag{3}$$

where $\lambda > 0$ ensures stable first-order dynamics.

The control input u(t) is designed to drive the system onto the surface and keep it sliding there (sliding condition). Accordingly, the control law is decomposed as follows

$$u(t) = u_{eq}(t) + u_{sw}(t) \tag{4}$$

where $u_{eq}(t)$ is the equivalent control that keeps the system on the surface by enforcing $\frac{d}{dt}s = 0$ (assuming no disturbance). The term $u_{sw}(t)$ is a discontinuous switching control that guarantees finite-time convergence of the system trajectories to the sliding surface and preserves the sliding condition. It is commonly defined as

$$u_{sw} = -K.sign(s(t)) \tag{5}$$

where sign(s(t)) is the signum function and $K > 0$ is a design gain.

In an IOBC, sliding mode control (SMC) can be applied to both the grid-connected front-end converter and the DC–DC converter that regulates battery charging. Primary control objectives include regulating output voltage and current, maintaining unity power factor, and mitigating the effect of grid or load disturbances. In [137], SMC is employed to control the current of the grid i_g and the voltage of the DC-link capacitor V_c. The errors in both quantities are fed to the SMC, which generates reference current and voltage signals while ensuring unity power factor operation.

To facilitate a concise, application-oriented comparison, Table 5 summarizes the key characteristics of the widely used control strategies for EV charging mode. From an automotive perspective, PI and PR controllers remain attractive due to their low computational burden and ease of real-time implementation. In contrast, MPC offers superior dynamic performance at the expense of significantly higher computational complexity. Intelligent control methods, such as fuzzy logic and sliding mode control, offer enhanced robustness and nonlinear handling capabilities but introduce additional implementation challenges, particularly on embedded automotive platforms with limited processing resources.

In summary, there is no strict one-to-one correspondence between IOBC topologies and control strategies; however, control selection is far from ad hoc. Instead, it is systematically governed by topological characteristics and, more critically, by the operating mode of the system. The charging mode control is largely standardized and grid-oriented due to CC–CV battery requirements and grid-compliance constraints, while the traction mode control offers greater flexibility to exploit machine and inverter capabilities for dynamic performance optimization. In contrast, V2G

operation imposes additional requirements related to bidirectional power flow, grid synchronization, ancillary service provision, and system-level protection, making control strategies predominantly topology- and mode-driven. Collectively, these considerations highlight that control strategy selection in IOBCs follows a clear, structured rationale aligned with functional objectives rather than arbitrary choice.

B. V2G MODE CONTROL SCHEMES

In vehicle-to-grid (V2G) operation, the IOBC transitions from a passive load to an active, grid-interactive power electronic interface, enabling bidirectional energy exchange between the vehicle battery and the utility grid. Unlike G2V charging, V2G control must simultaneously satisfy vehicle-level constraints—such as battery state-of-charge limits, degradation, and torque-free operation—while meeting grid-side requirements, including synchronization, power-quality compliance, and the provision of ancillary services. Consequently, V2G control extends beyond local current regulation to encompass coordinated active and reactive power control, grid support functions, and system-level energy management, positioning IOBCs as distributed energy resources within modern smart grid architectures.

1) GRID SYNCHRONIZATION AND PLL DESIGN

In V2G systems, grid synchronization is a fundamental requirement for the safe and stable operation of grid-connected EV chargers. Accurate estimation of the grid voltage phase and frequency directly affects current control precision, bidirectional power transfer, and compliance with grid codes. Unlike conventional grid-tied converters, V2G converters face unique challenges due to intermittent EV connections, rapid plug-in/plug-out events, and simultaneous charging/discharging of multiple vehicles, which can induce voltage fluctuations, harmonics, and unbalanced conditions.

The PLL remains the primary tool for grid synchronization in EVs. A typical PLL consists of three core components: a phase detector, a loop filter, and a voltage-controlled oscillator, enabling accurate tracking of the phase and frequency of the grid [138], [139], [140]. Among the various PLL techniques, the synchronous reference frame PLL (SRF-PLL) is widely adopted in EVs due to its simple structure, ease of digital implementation, and reliable performance under nominal grid conditions [141]. However, the SRF-PLL may exhibit degraded dynamic performance under weak-grid conditions or in the presence of voltage harmonics and unbalances, leading to phase oscillations, frequency estimation errors, and potential instability during bidirectional power transfer.

To address these challenges, advanced PLL structures have been proposed for V2G applications. Techniques such as the Decoupling Synchronous Reference Frame PLL (DSRF-PLL), Decoupling Double Synchronous Rotating Frame PLL (DDSRF-PLL), and Dual Second-Order Generalized Integrator PLL (DSOGI-PLL) improve robustness against harmonics, unbalanced voltages, and weak-grid conditions. These PLLs ensure fast, accurate synchronization, which is particularly important during EV plug-in events and during dynamic power reversals during Vehicle-to-Grid operation. Proper PLL design and tuning are therefore essential not only for current control stability and power quality, but also for enabling reliable, safe, and efficient integration of EVs into the grid.

2) ACTIVE AND REACTIVE POWER CONTROL (P–Q CONTROL)

EVs can be connected to the grid in V2G mode and act as an energy source to the grid. In this mode, the main objectives of the controllers are to regulate the power, i.e., active and reactive, between the EVs and the power grid. The reference for these power exchanges is set by the higher energy management system based on objectives such as charging scheduling, grid support, or frequency regulation, while the reactive power reference is used to provide voltage support and improve power factor at the point of common coupling. This active power command is translated into a d-axis current reference i_d^*, which directly governs the real power exchanged when the reference frame is aligned with the grid voltage vector. The q-axis current reference i_q^* is derived from reactive power or voltage support objectives and depends on grid code requirements, common-coupling point, voltage deviations, and power factor constraints.

To fulfill these objectives, PI controllers in the synchronous reference frame are commonly employed because they can decouple the dynamics of active and reactive power [142]. Typically, an outer-loop active power, DC-link voltage, or frequency controller generates i_d^*, while a reactive power or voltage controller produces i_q^*. More advanced control strategies, such as MPC [143], [144] and adaptive current regulators, have been investigated to enhance dynamic performance under weak-grid conditions and during rapid transitions between charging and discharging in V2G operation.

3) ISLANDING DETECTION AND PROTECTION MECHANISMS

Islanding detection and protection are critical requirements for V2G systems to ensure safe operation and compliance with grid codes during abnormal grid conditions. Islanding occurs when the utility grid is unintentionally disconnected while the grid-connected converter continues to energize the local load, potentially posing safety risks to utility personnel and connected equipment. In a V2G control scheme, rapid and reliable islanding detection is therefore essential to prevent sustained operation in an unintentional islanded state.

Both passive and active islanding detection methods are commonly employed in V2G-enabled converters. Passive techniques monitor grid parameters such as voltage magnitude, frequency, rate of change of frequency, and phase angle deviations at the point of common coupling, triggering disconnection when predefined thresholds are exceeded [145],

[146], [147], [148]. However, their effectiveness is limited by non-detection zones under closely matched load–generation conditions. To address this limitation, active methods deliberately introduce small perturbations in the converter output—such as reactive power injection, frequency drift, or phase modulation—and observe the grid response to distinguish between grid-connected and islanded operation [149], [150]. Hybrid approaches that combine passive monitoring with active probing are often adopted in V2G systems to achieve fast detection while minimizing power quality degradation.

Upon islanding detection, the V2G controller initiates protection actions in accordance with grid standards, including immediately ceasing power injection, opening the grid-side contactor, and transitioning to a safe operating state. In advanced implementations, the control scheme may also support seamless mode transitions, allowing the converter to switch to local voltage or power control for intentional islanding or microgrid operation. These protection mechanisms ensure operational safety, regulatory compliance, and robust interaction between V2G systems and the utility grid.

4) MODE TRANSITION AND SUPERVISORY CONTROL

Mode transition and supervisory control form the system-level energy management layer in V2G-enabled IOBC systems, coordinating power flow between the vehicle battery, the grid, and external energy resources to ensure safe, efficient, and resilient operation. A V2G-enabled charger typically operates in multiple modes, such as G2V charging, V2G discharging, standby, and fault or protection modes. The supervisory controller monitors system-level variables such as grid availability and quality, battery state of charge (SoC), thermal limits, user commands, grid support requests, and protection signals, and selects the appropriate operating mode and power references.

From an energy management perspective, the supervisory layer translates high-level objectives—such as RE utilization, peak shaving, cost minimization, and ancillary service provision—into active and reactive power commands for lower-level controllers. During transitions between G2V and V2G modes, it manages reference ramping, current limiting, and synchronization to prevent transient overcurrents, DC-link voltage excursions, and grid disturbances. Smooth transitions are typically achieved through coordinated adjustment of power references while maintaining phase synchronization via the PLL, with state-machine and hysteresis-based logic used to avoid frequent mode switching.

The supervisory controller also enables grid-interactive and resilient operation by coordinating multiple energy assets and responding to system-level disturbances. Recent studies demonstrate that optimal supervisory scheduling of EV charging, discharging, and auxiliary resources—such as photovoltaic generation, stationary energy storage, and hydrogen refueling infrastructure—significantly improves operational efficiency and resilience under dynamic grid conditions [151]. Similarly, integrated energy management of EV parking facilities with regenerative energy sources and storage systems enhances the utilization of renewable energy while maintaining grid stability [152].

In addition, the supervisory layer coordinates protection and fault-handling actions, including islanding detection, grid fault response, and enforcement of battery protection, ensuring compliance with grid codes and automotive safety standards. In advanced V2G architectures, it may interface with aggregators or higher-level energy management systems to enable coordinated multi-vehicle ancillary services. This hierarchical structure, which separates fast inner-loop current control from slower system-level decision-making, is essential for scalable, grid-interactive, and resilient IOBC and V2G operation.

5) SAFETY, STANDARDS, AUTOMOTIVE CONSTRAINTS, AND GLOBAL DEPLOYMENT OF V2G SYSTEMS

Compliance with safety and standards is a fundamental consideration in the design of V2G control schemes, as the system interfaces both automotive battery packs and utility power networks. From an automotive perspective, the control architecture must enforce strict battery protection constraints, including limits on voltage, current, temperature, and SoC, to prevent degradation and ensure long-term reliability. These constraints directly influence the allowable charging and discharging power levels, the generation of current references, and mode transitions during V2G operation.

On the grid side, V2G converters must comply with international standards and grid codes, such as IEEE 1547, IEC 61851, ISO 15118, IEC 61850, and regional low-voltage ride-through and power-quality requirements. Compliance requires accurate control of active and reactive power, harmonic distortion, and fault response, including anti-islanding protection and controlled disconnection during abnormal grid conditions. The control scheme must therefore integrate protection mechanisms and limit enforcement within the supervisory layer to ensure coordinated and fail-safe operation.

In addition to electrical standards, automotive constraints, such as limited onboard computational resources, electromagnetic compatibility, and functional safety requirements (e.g., ISO 26262), further shape the V2G control design. These constraints favor control strategies with predictable behavior, bounded computational complexity, and robust fault handling. Consequently, V2G control schemes often adopt hierarchical architectures that separate fast inner-loop current control from slower supervisory and energy management functions, allowing compliance with both grid regulations and automotive safety standards while maintaining reliable bidirectional operation.

Despite these constraints, practical demonstrations worldwide indicate that V2G deployment is technically feasible and continues to progress steadily. In recent years, thousands of bidirectional charging points have been installed across numerous countries, supporting a growing number of pilot

and demonstration projects. Europe currently represents one of the leading regions in terms of deployment activity, with the United Kingdom hosting a significant portion of these initiatives. At the same time, the United States and several Asian countries have also developed advanced V2G trials that are integrated with grid services such as frequency regulation and peak shaving.

China has emerged as a particularly active region in recent years. Several large-scale initiatives have been introduced, including the integration of V2G capabilities into peak-shaving and ancillary service markets by major grid operators, the commissioning of advanced V2G-enabled charging stations, and the development of public demonstration projects incorporating bidirectional charging and battery-swapping technologies. These developments demonstrate that V2G operation under real grid conditions and within existing regulatory frameworks is both feasible and increasingly practical.

V. OPERATIONAL CHALLENGES IN IOBCs

Although IOBCs offer significant advantages, such as high-density power transfer with greater utilization of machine components, compact size, high efficiency, low cost, and charging flexibility. They also pose some challenges when connected to the grid. These challenges, if not adequately mitigated, could cause problems during EV charging. These challenges have appeared mainly in the form of unnecessary torque production during charging due to the utilization of machine windings as a charging component, torque and current ripples that are generated due to the switching action of power switches, EMI issues related to these chargers, and thermal management of these chargers that arise due to overheating of the charger's components.

A. TORQUE PRODUCTION

The unconventional use of machine windings as an inductor requires full consideration of electromagnetic analysis and a dedicated control scheme. Because machine windings create a rotating electromagnetic phenomenon that tends to cause the rotor to rotate during charging time [26]. Therefore, during EV charging, the average electromagnetic torque must be zero, and any residual torque ripple must remain extremely small to prevent rotor movement, vibration, or safety issues. Although no explicit numerical limit is defined in public standards, industry practice typically restricts the charging torque to well below 1–2% of the rated torque, with even stricter limits set by OEMs. This requirement is enforced by installing a parking brake with an appropriate locking torque if the torque cannot be reduced during the charging process. There is also the possibility that the machine shaft must be decoupled from the transmission system using a clutch, which increases the system's cost and complexity. The other option is to use a control scheme that uses the machine current to produce zero-average torque during charging.

Different authors suggest different techniques to overcome this challenge; for example, the authors in [24] suggest that the charging torque will be zero if the torque produced by the space vector current is equal and opposite to that produced by the homopolar current during charging mode. The current flowing through the three-phase windings of the PMSM, if balanced in both magnitude and phase, results in torque cancellation during charging mode under the condition that the harmonic current is not so high [117], [119], [135]. Similarly, the rotor is displaced from its original position to the nearest zero-torque charging position, which provides equal and opposite torques so that the net torque is zero [16], [118], [153], [154], [155]. A decoupled current control is used to control the q-axis current of the PMSM in [110], thereby controlling the charging torque during the vehicle charging mode. The winding arrangement in [156] results in the cancellation effect of the magnetic field, which results in a zero charging torque. This is because the machine's alpha-beta current forms a straight-line pulse; hence, it does not produce a rotating magnetic field, which would cause the rotor to rotate during charging time. A standstill position of the vehicle during charging mode can also be achieved at any rotor position by making the q-component of the stator current equal to zero. Further, to reduce peak current, a scaling factor is introduced that reduces them at the maximum torque rotor position. In a PMSM, the total torque is the sum of magnetic and reluctance torque; therefore, if these two torques are equal and opposite during charging mode, the average total torque becomes zero. This can be achieved by making $i_d > 0$ and letting the magnetizing current lie on the trajectory formed from the zero-torque locus, which can be obtained by crossing the first and fourth quadrants of the dq-plane [102]. In addition, some researchers have suggested using the concept of a zero-torque hyperbola in the current plane, based on only two phases of the stator windings of a three-phase PMSM [124]. The authors leverage this concept to define a current trajectory where the electromagnetic torque becomes zero, despite the presence of permanent magnets. This is achieved by choosing different combinations of two phases of stator currents, such as $a\&b$, $b\&c$, and $c\&a$, which yield an equilateral triangle in the $\alpha\beta$ plane. The intersection of the torque hyperbola plane and the equilateral triangle defines the zero-torque points.

B. GENERATION OF CURRENT AND TORQUE RIPPLES

One main challenge associated with charging an EV accompanied by an IOBC is the generation of torque and current ripples during charging. Unwanted current and torque ripples can arise from several factors, including the switching action of the converter power switches, the motor winding's pulsating current during charging, zero-sequence circulating current flow, motor phase interaction, and the charger's imperfect decoupling between charging and propulsion states. Various researchers have proposed solutions to mitigate these ripple issues in the literature.

The interleaved PWM technique has been used to reduce ripples in the output current of the machine and the current

towards the grid during V2G mode [108], [122], [124], [124]. In [127], a buck converter equipped with an LC circuit was used to suppress second-order power oscillations arising from rectifier switching. The ripples are generated at the DC-link side at twice the line frequency, which, if not removed, could cause additional Joule loss and may damage the equipment. Similarly, some researchers focused on using a smoothing filter and a high switching frequency to mitigate charging current ripples, as mentioned in [26] and [116]. Due to magnetic saturation, the winding inductance of the machine changes, causing corresponding variations in winding current ripple. When inductance decreases, the current ripple increases, leading to greater power losses and increased noise. Mitigation strategies include adding an external inductor to the system, which increases both cost and volume, or adjusting the switching frequency. To suppress current ripples, the selection of the switching frequency relative to winding inductance is performed to ensure that the THD of the grid current remains below 5% at nominal power output [117], [118]. Single-phase charging systems inherently generate power ripple on the DC side at twice the grid frequency, which increases battery temperature and accelerates battery degradation. To mitigate this issue, some researchers have proposed a motor winding configuration in which two windings are connected in parallel and utilized as a grid-interface inductance for the traction inverter. The challenge of suppressing the 100 Hz harmonic ripple on the DC bus is addressed through a ripple-power cancellation technique that employs an energy-storage inductor. In this approach, the motor's third winding serves as the energy-storage inductor for active power decoupling, eliminating the need for additional external components [110].

C. THERMAL MANAGEMENT

Due to the growing demand for high charging currents to enable fast charging, effective thermal management has become critically important in IOBCs. In addition, the high switching frequency and compact structure of IOBCs further underscore the need for an effective thermal management system, as the skin effect and eddy-current losses in the power switching devices generate significant heat. A well-designed thermal management technique is needed to protect the switching devices, ensure safe and reliable operation, and achieve good charger performance.

Two primary thermal management techniques are commonly employed: air cooling and liquid cooling. In air cooling, heat is dissipated from component surfaces through natural or forced convection. This method may be supplemented by heat sinks or fans to enhance airflow and improve heat dissipation. It is typically used for components with moderate thermal loads. However, liquid cooling involves circulating a liquid coolant over or near heat-generating components, i.e., switching devices, magnetic components, machine windings, and battery packs. The coolant absorbs heat and transports it away from the device, where it is expelled into the environment. Liquid cooling is generally reserved for high-temperature components due to its superior heat extraction capability [157], [158].

In [159], the authors analyzed the use of liquid-cooling plates with water-glycol coolant for the thermal management of EV chargers. Two methods are studied, using simulation and experimental tests, for the thermal management of switching devices and magnetic components. For power switching devices, liquid cooling is typically employed, whereas magnetic components are cooled using recirculated air and potted magnetic structures. Some researchers propose hybrid cooling systems that combine two-phase heat pipes with single-phase liquid cooling to address the thermal challenges of EV components such as the battery, inverter, and motor [160]. A heat-pipe-based forced air-cooling system for silicon carbide (SiC) traction inverters in EVs has been discussed in [161]. Using U/L-shaped copper-water heat pipes and aluminum fin stacks, it manages asymmetric heat fluxes (up to 17 W/cm^2) while maintaining junction temperatures $< 142°C$ (below $175°C$ limit).

The thermoelectric cooling (TEC) approach is also used for thermal management in power electronics, actively regulating device temperatures—particularly those of IGBTs—under varying load conditions. By modulating the TEC current, the system reduces thermal cycling by up to $30°C$ versus passive methods [162]. TEC systems, in combination with heat pipe exchangers, enhance the thermal control of power electronic devices. The system leverages the Seebeck effect to convert waste heat from electronic components into electricity, which powers a fan to improve forced convection—eliminating the need for external power [163]. Although TEC systems introduce an additional 5–15% power loss, they provide precise thermal regulation, improve reliability, and extend component lifespan in EV and RE applications [162].

D. ISOLATION AND SAFETY REQUIREMENTS

In IOBCs, where the electric drive and charging system share common hardware components, such as motor windings or a DC-link, ensuring electrical isolation and user safety becomes more challenging than in isolated on-board chargers. When the vehicle is connected to the high-voltage charging station, a high-voltage pathway is created between the grid and the vehicle's low-voltage components. Thus, a line-frequency transformer is needed to galvanically isolate the EV low-voltage components from the high-voltage AC grid. However, the line-frequency transformer, with its large size and volume, significantly increases the cost of the charging station. To solve this issue, a high-switching-frequency, galvanically isolated DC-DC converter stage is introduced into the charging circuit. A detailed discussion of the different techniques and topologies used in isolated IOBCs has already been presented in section III. Furthermore, leakage currents caused by the common-mode voltage of the power converter must be mitigated for safety. Compliance with relevant international standards is therefore required to ensure user safety during EV charging.

The standard IEC61851-1 [164] describes the safety requirements that ensure protection against electric shock, overcurrent, and thermal hazards. These standards emphasize galvanic isolation, ground-fault detection, and a secure communication protocol between the EV and the grid. According to IEC 61140 [165], IOBCs must comply with stringent insulation, isolation, and fault-protection criteria to ensure user safety against electric shock. This includes coordination of insulation, protective grounding, and separation of control and power circuits. These requirements become even more critical in integrated systems where traction and charging share hardware paths, increasing the risk of fault propagation. Similarly, IEC60990 [166] defines the earth-leakage and contact-limit current that flows through the body of the vehicle. These standards set the limit of this current to be 3.5 mA for a sinusoidal current having a frequency of 50 Hz.

In this section, a comprehensive assessment of IOBC challenges has been conducted, considering key factors such as charging torque and current, torque ripple minimization, thermal performance, and compliance with isolation and safety standards for grid-connected systems. The detailed classification of challenges, their causes, consequences, and possible solutions is presented in Table 6.

VI. FUTURE RESEARCH OPPORTUNITIES

Over the past decade, the number of EVs has increased significantly [5], highlighting the increasing importance of charging systems and infrastructure. For EV users, fast, convenient, and accessible charging is a critical requirement, while vehicle range remains a key consideration for long-distance travel [170]. Charging solutions, whether integrated within the vehicle [171] or provided externally through stations [172], employ different operating principles and strategies. Residential chargers typically offer lower power density, resulting in longer charging times, but they benefit from ease of access. In contrast, commercial fast DC chargers offer high power density and reduced charging times but face challenges with grid integration and limited availability [15]. A promising approach is to enhance the power density and efficiency of widely accessible Level 1 and Level 2 chargers. The use of EV machine windings and a shared power converter for both traction and charging—known as IOBCs—can significantly improve cost, efficiency, and power density. However, in IOBCs, the main technical challenges are associated with charging torque minimization, current ripple reduction, thermal management, and ensuring isolation and safety. Therefore, this section highlights key areas where research and technological improvements are needed to advance integrated charging solutions.

Table 7 presents a qualitative assessment of research gaps across six key domains of IOBCs, namely power converter topologies, IOBC optimization, control strategies, thermal management, energy storage integration, renewable and grid interaction, and cybersecurity and resilience. Each domain is evaluated against five system-level criteria—research effort, technical challenges, potential impact, technological maturity, and practical feasibility—using qualitative ratings ranging from Low to Very High. The comparative analysis highlights domains that exhibit high potential impact but limited maturity, such as cybersecurity and grid resilience, as well as areas where substantial research effort has already been devoted, including power converter topologies and control strategies. By providing a structured and transparent comparison, the table enables clear identification of priority research directions and unresolved challenges, thereby guiding future developments in IOBC technologies and EV charging systems.

A. POWER CONVERTER TOPOLOGIES

Power converters play a critical role in both integrated and non-IOBC architectures. As discussed earlier, a variety of topologies have been explored in the literature, encompassing both isolated and non-isolated configurations.

In the case of isolated OBCs, galvanic isolation offers several key advantages, including enhanced operational safety, compliance with international standards, improved fault tolerance, and superior electromagnetic compatibility (EMC) performance. Traditionally, this isolation has been implemented using line-frequency transformers (LFTs). However, LFT-based solutions suffer from significant drawbacks, such as high cost, large physical volume, low power density, and reduced efficiency due to core and copper losses at low operating frequencies.

To address these limitations, recent research has shifted toward replacing LFTs with solid-state transformers (SSTs). SST technology leverages high-frequency power electronic conversion stages and a high-frequency isolation transformer to achieve galvanic isolation while significantly reducing size and weight. With switching frequencies in the tens to hundreds of kHz range, SSTs can drastically shrink magnetic cores, which increases power density and efficiency while enabling finer dynamic control, especially under partial-load conditions. Additionally, SSTs provide flexible voltage regulation, bidirectional power flow capability, and easier integration with energy storage systems and V2G applications [173], [174], [175], [176].

B. IOBC IMPROVEMENT

The IOBC offers a promising approach to EV charging by reconfiguring existing traction-drive components to perform the charging function. This integration can potentially enable higher charging power and improved efficiency compared to non-integrated counterparts, although the actual charging rate remains dependent on grid capacity, battery specifications, and thermal limits. Despite these advantages, several aspects require further research and optimization. Key areas include minimizing Joule losses caused by using machine windings as both boost and filter inductances [124], and improving the reliability of power electronic devices subjected to continuous operation in both charging and traction modes. Furthermore, a detailed investigation of charging torque

TABLE 6. Challenges with IOBC Topologies.

Ref.	Challenge category	Causes	Impacts	Potential solutions
[16], [24], [26], [102], [109], [117], [119], [124], [153]-[156]	Charging Torque	Flow of currents in the machine windings (Integrated charger)	Instability, oscillations and vibrations, mechanical stress and bearing wear, thermal effects, efficiency degradation	Parking brake, making overall torque zero, balanced current flow, displacement of rotor to nearest zero torque position, decouple control of iq, winding arrangement of machine.
[26], [108], [116], [117], [124], [127]	Torque and current ripples	Switching action of the switches, PWM effects, interaction between charging and traction modes, imperfect filtering and compensation, magnetic saturation and core Losses	Mechanical stress and vibration, efficiency losses, thermal stress and hot spots, EMI and harmonic distortion, control and stability issues	Variable switching frequency, interleaving PWM, LC filter, smoothing reactor, high switching frequency
[157]-[163], [167]-[169]	Thermal issues	High conduction losses, switching loss, core losses, compactness or less area for heat dissipation, ambient and environmental factors, faults	Efficiency reduction, components aging, reliability degradation, parameter variation of machines, safety and derating of performance	Use of wide-band gap switching devices, improvement in cooling techniques (liquid cooling), control strategy optimization for effective joule loss management, enhance PCB design
[164]-[166]	Isolation and safety requirements	Share of common hardware components, high voltage pathway, issue of leakage current, Fault condition	Components failure, battery damage, thermal stress and aging, electric shock, fire and arch flash risk, uncontrolled fault current	Galvanic isolation, leakage and ground fault protection, proper earthing and grounding, compliance with standards, fault-tolerant topology

TABLE 7. Qualitative assessment of research gaps in IOBCs.

Research Area	Research Effort	Challenges	Potential Impact	Maturity	Feasibility
Power converter topologies	Very High	Medium	High	Medium-High	High
IOBC optimization	High	High	Very High	Medium	Very High
Control strategies	High	High	Very High	Medium-High	High
Thermal management	Medium	Very High	High	Low-Medium	High
Energy storage integration	Medium-High	Medium-High	High	Medium	Medium
Renewable and grid integration	High	Very High	Very High	Low–Medium	Medium
Cybersecurity and resilience	Medium	Very High	Very High	Low	Medium

generation and effective mitigation techniques is essential. Although the dual use of machine windings for charging and traction can significantly reduce the overall system size, it also poses notable thermal management challenges, especially when targeting high power density (power per unit volume).

C. USE OF WIDE-BANDGAP DEVICES

Wide-bandgap (WBG) semiconductor devices, such as silicon carbide (SiC) [177] and gallium nitride (GaN) [178], offer significant advantages over conventional silicon devices, making them particularly suitable for IOBC applications. Their higher efficiency, faster switching capability [179], and ability to operate at high voltages and temperatures [167] enable more compact, lighter, and thermally efficient charger designs [180], [181]. Recently, it has been observed that the use of WBG devices by different EV owners has increased tremendously. For IOBCs, these characteristics can be leveraged to increase power density [182], reduce losses, support higher switching frequencies, and minimize the size of passive components—factors that directly address key bottlenecks in current IOBC technology.

However, despite these promising attributes, the practical integration of WBG devices into IOBC architectures remains underexplored. Challenges such as managing EMI at higher switching frequencies, ensuring long-term device reliability under continuous dual-mode operation (charging and traction), developing cost-effective thermal management solutions for high power densities, and optimizing converter topologies for both efficiency and isolation remain largely

unaddressed. Moreover, existing studies often focus on component-level improvements without providing a holistic, system-level design methodology that simultaneously considers electrical performance, thermal constraints, EMI suppression, and cost-effectiveness [183].

D. THERMAL MANAGEMENT SYSTEM

In the context of IOBCs, thermal management remains a critical area that requires further exploration, particularly as power density, efficiency, and multifunctional integration continue to advance. Future research should investigate innovative cooling techniques that can effectively handle the concentrated heat generated by power electronics, magnetics, and control circuits within a compact enclosure, especially when these components are shared between traction and charging functions. This includes the development of advanced liquid cooling architectures [157], [158], [159], hybrid cooling systems [160], forced air-cooling [161] and TEC methods that minimize thermal resistance [162], [163]. More research is required on the interaction between the OBC and the vehicle's existing thermal circuits, including the motor and battery cooling systems, to enhance energy efficiency and thermal stability without adversely affecting other subsystems. Additionally, researchers should focus on predictive thermal modeling and real-time thermal monitoring strategies to enable intelligent thermal control that dynamically adjusts operating conditions to prevent overheating while maximizing performance. With the trend toward higher switching frequencies and WBG semiconductor devices such as SiC and GaN, the thermal characterization of these devices under varying load and environmental conditions also warrants a detailed investigation [167]. Furthermore, material research—such as advanced thermal interface materials, phase change materials, and high-performance heat sink designs [168], [169]—can significantly improve heat dissipation in IOBCs. Finally, reliability studies addressing thermal cycling, hotspot formation, and long-term degradation under combined traction and charging operations will be essential to ensure that IOBC systems meet the demanding durability standards of future EVs.

E. CONTROL SYSTEM IMPROVEMENT

In IOBCs, the design and optimization of controllers and control systems are critical for achieving high efficiency, fast dynamic response, and safe operation across varying grid and battery conditions. Future research should focus on developing advanced control strategies that can manage multiple functions simultaneously, such as AC/DC conversion, DC/DC regulation, bidirectional power flow, and active power decoupling, all within a compact integrated architecture. Intelligent control algorithms, including MPC [109], [118], [130], [131], Fuzzy control [132], [133], [134], [135], [136], and robust sliding-mode techniques [137], can be explored to handle nonlinearities, parameter variations, and transient conditions while maintaining precise voltage and current regulation. The integration of WBG devices further necessitates control strategies that exploit their fast switching capabilities without introducing excessive EMI or instability. Real-time monitoring, fault detection, and predictive control are also key areas that enable the system to respond quickly and reliably to overvoltage, overcurrent, thermal excursions, or grid disturbances. In addition, control systems must be designed to ensure smooth transitions between charging modes, bidirectional operation for V2G applications, and compliance with grid codes, while optimizing efficiency and minimizing stress on the battery. Finally, the co-design of control algorithms with hardware, including power stages and passive components, is essential to fully leverage the potential of IOBCs and to achieve robust, high-performance, and compact charging solutions suitable for next-generation EVs.

F. ENERGY STORAGE SYSTEM

For ESS in IOBCs, future research must address several interconnected challenges related to efficiency, safety, and system longevity [87], [93], [94], [95]. One key area is the optimization of the battery–charger interface, where control strategies, charging profiles, and balancing methods must be refined to minimize cell stress while enabling fast charging. With IOBCs operating in both propulsion and charging modes, bidirectional power flow introduces additional thermal and electrical stress on the ESS, making an advanced BMS essential for real-time monitoring, fault detection, and adaptive control. Furthermore, integration with IOBCs demands research into the impact of high-frequency switching, harmonics, and ripple currents on battery degradation, as excessive ripple can accelerate aging and reduce capacity over time. The thermal management of the ESS is equally critical, requiring new approaches to dissipate heat during high-rate charging while maintaining a uniform temperature distribution across cells to avoid hotspots and imbalance [184], [185]. The interaction between ESS and RE sources, along with V2G functionalities, creates opportunities for predictive control and energy scheduling to maximize efficiency while protecting battery health. In addition, advances in solid-state batteries, hybrid storage systems [186], [187], and ultracapacitor integration may redefine how future IOBCs interface with energy storage, necessitating new control algorithms, protection schemes, and state-of-health estimation methods that can adapt to evolving battery chemistries. Overall, the ESS in IOBCs is not just a passive energy reservoir but a dynamically managed component whose performance and longevity will increasingly depend on intelligent, adaptive, and thermally aware integration strategies.

G. INTEGRATION OF RE RESOURCES AND CONCEPT OF SMART GRID

In the context of IOBCs, integrating RE resources and adopting Smart Grids presents both opportunities and challenges that require further research [188], [189]. Future IOBC designs must be capable of interfacing seamlessly with variable and distributed renewable sources, such as solar

photovoltaics and wind energy, which not only introduce fluctuations in voltage and frequency, but also compromise power quality and stability [57], [58], [59], [60], [61]. Advanced control strategies are needed to manage these variations while maintaining stable and efficient charging of the EV battery. The concept of a smart grid extends this requirement by enabling bidirectional communication and power flow between the vehicle and the grid, allowing for V2G [190] and vehicle-to-home (V2H) [191] operations. This requires the IOBC to support real-time energy management, demand response, and grid ancillary services, while ensuring compliance with grid codes and maintaining the safety and health of the battery [67]. Additionally, predictive algorithms, artificial intelligence, and machine learning can be explored to optimize charging schedules, minimize energy costs, and maximize RE utilization. Integration of IOBCs with Smart Grids and RE systems also raises the need for robust fault detection, cybersecurity measures, and adaptive control to handle dynamic grid conditions, voltage sags, and power quality issues. Overall, future research should focus on creating IOBC architectures that are not only efficient and compact but also intelligent and flexible enough to interact dynamically with RE sources and smart grid infrastructures.

H. CYBER SECURITY AND DATA-DRIVEN RESILIENCE IN EV CHARGING SYSTEMS

Despite notable advances, cybersecurity and resilience in EV charging and V2G-enabled systems remain open research challenges, particularly at the system level. Existing studies predominantly focus on attack detection, while comprehensive threat modeling and post-attack recovery strategies, essential for maintaining grid stability and service continuity, are still insufficiently addressed [192]. Recent work has begun to explore data-driven and AI-based resilience frameworks, such as generative self-supervised learning for cyberattack-resilient EV charging demand forecasting and transformer-based multi-feature fusion approaches for resilient charging monitoring systems, demonstrating the potential of advanced learning architectures for enhancing robustness under adversarial conditions [193], [194]. However, broader challenges persist, including limited consideration of EV user behavior as a source of vulnerability, insufficient assurance of AI models (e.g., explainability and robustness), and weak resistance to adversarial and model-poisoning attacks [195]. Furthermore, blockchain- and encryption-based V2G cybersecurity solutions often suffer from scalability issues, high computational overhead, and a lack of real-world validation, while quantum-safe security mechanisms remain largely unexplored [196], [197], [198], [199]. Addressing these gaps requires integrated, multi-layer cybersecurity frameworks that combine adaptive and explainable AI, resilient control and optimization strategies, scalable blockchain architectures, and quantum-resistant cryptography, thereby enabling secure, grid-interactive, and resilient operation of future IOBC- and V2G-enabled EV ecosystems [200], [201].

VII. CONCLUSION

This article presents a comprehensive review of IOBCs for EVs, summarized as follows.

- Conventional off-board charging stations impose high infrastructure costs, raise grid stability concerns, and present difficulties in RE integration. IOBCs offer a viable alternative by reducing system size, weight, and cost while improving flexibility.
- Both isolated and non-isolated IOBC topologies have been examined. Isolated solutions ensure safety and grid compliance but suffer from reduced efficiency and increased complexity. In contrast, non-isolated architectures offer higher efficiency and compactness but pose challenges in achieving reliable isolation and safety compliance.
- Various control strategies have been implemented in IOBCs to regulate charging performance and grid interaction. Each class of controllers offers trade-offs in simplicity, computational demand, and robustness. Although conventional linear controllers remain popular for industrial adoption, advanced nonlinear and predictive approaches demonstrate promising potential to enhance dynamic response and efficiency.
- Key technical barriers remain in the deployment of IOBCs, including torque generation during charging, current and torque ripple, thermal management, and strict isolation and safety requirements. These issues must be addressed to ensure reliable operation without compromising vehicle drivability or passenger safety.
- Emerging research directions include the development of innovative converter architectures, the adoption of WBG devices to achieve higher efficiency and power density, advances in thermal management and control strategies, enhanced cybersecurity and system resilience, and seamless integration with RE sources and Smart Grid infrastructures. These efforts are essential for transitioning IOBCs from laboratory prototypes to large-scale commercial deployment.

Taking the above findings into account, IOBCs represent a transformative step towards high-efficiency, cost-effective charging for EVs. Although significant advancements have been made in topology development and control design, further research is essential to overcome persistent challenges and align IOBC technology with the evolving requirements of electrified transportation and future Smart Grids.

REFERENCES

[1] J. Domone, "The challenges and benefits of the electrification of aircraft," SNC Lavalin, Montreal, QC, Canada, Tech. Rep., Jun. 2018 [Online]. Available: https://www.atkinsrealis.com/~/media/Files/A/atkinsrealis/download-centre/en/whitepaper/electrification%20white%20paper%20-%20digital.pdf4

[2] S. Wang and M. Ge. (Oct. 2019). *Everything You Need to Know About the Fastest-Growing Source of Global Emissions: Transport*. World Resources Institute. [Online]. Available: https://www.wri.org/blog/2019/10/everything-youneed-know-about-fastest-growing-source-global-emissions-transport

[3] U.S. Environmental Protection Agency (EPA). *Sources of Greenhouse Gas Emissions in the USA*. Accessed: Sep. 15, 2022. [Online]. Available: https://www.epa.gov/ghgemissions/sources-greenhouse-gas-emissions

[4] P. Jaramillo, S. Kahn Ribeiro, P. Newman, S. Dhar, O. E. Diemuodeke, T. Kajino, D. S. Lee, S. B. Nugroho, X. Ou, A. H. Strømman, and J. Whitehead, "Transport," in *Climate Change 2022—Mitigation of Climate Change*. Cambridge University Press, 2023, pp. 1049–1160. [Online]. Available: https://doi.org/10.1017/9781009157926.012

[5] IEA. (2024). *Global Electric Vehicle Stock By Region*. [Online]. Available: https://www.iea.org/reports/global-ev-outlook-2025

[6] F. Michael, K. Mathias, S. Rohr, S. Schickrama, M. Sinninga, and M. Lienkamp, "An overview of costs for vehicle components, fuels, greenhouse gas emissions total cost ownership update 2017," pp. 1–19, 2017. [Online]. Available: https://www.researchgate.net/publication/260339436_An_Overview_of_Costs_for_Vehicle_Components_Fuels_and_Greenhouse_Gas_Emissions

[7] M. Yilmaz and P. T. Krein, "Review of battery charger topologies, charging power levels, and infrastructure for plug-in electric and hybrid vehicles," *IEEE Trans. Power Electron.*, vol. 28, no. 5, pp. 2151–2169, May 2013.

[8] S. S. G. Acharige, M. E. Haque, M. T. Arif, N. Hosseinzadeh, K. N. Hasan, and A. M. T. Oo, "Review of electric vehicle charging technologies, standards, architectures, and converter configurations," *IEEE Access*, vol. 11, pp. 41218–41255, 2023.

[9] Y. S. Rutia, I. Vajpai, and J. Vajpai, "Comparative performance analysis of electric motors for vehicle propulsion: Why PMSMs lead the charge," in *Proc. Int. Conf. Adv. Renew. Energy Electric Vehicles (AREEV)*, Feb. 2025, pp. 1–7.

[10] O. Bay, M. Tran, M. El Baghdadi, S. Chakraborty, and O. Hegazy, "A comprehensive review of GaN-based bi-directional on-board charger topologies and modulation methods," *Energies*, vol. 16, no. 8, p. 3433, Apr. 2023.

[11] H. Karneddi, D. Ronanki, and R. L. Fuentes, "Technological overview of onboard chargers for electrified automotive transportation," in *Proc. IECON – 47th Annu. Conf. IEEE Ind. Electron. Soc.*, Oct. 2021, pp. 1–6.

[12] D. Yildirim, S. Öztürk, I. Çadirci, and M. Ermis, "All SiC PWM rectifier-based off-board ultrafast charger for heavy electric vehicles," *IET Power Electron.*, vol. 13, no. 3, pp. 483–494, Feb. 2020.

[13] M. A. H. Rafi and J. Bauman, "A comprehensive review of DC fast-charging stations with energy storage: Architectures, power converters, and analysis," *IEEE Trans. Transport. Electrific.*, vol. 7, no. 2, pp. 345–368, Jun. 2021.

[14] J. Yuan, L. Dorn-Gomba, A. D. Callegaro, J. Reimers, and A. Emadi, "A review of bidirectional on-board chargers for electric vehicles," *IEEE Access*, vol. 9, pp. 51501–51518, 2021.

[15] H. Tu, H. Feng, S. Srdic, and S. Lukic, "Extreme fast charging of electric vehicles: A technology overview," *IEEE Trans. Transport. Electrific.*, vol. 5, no. 4, pp. 861–878, Dec. 2019.

[16] Y. Xiao, C. Liu, and F. Yu, "An effective charging-torque elimination method for six-phase integrated on-board EV chargers," *IEEE Trans. Power Electron.*, vol. 35, no. 3, pp. 2776–2786, Mar. 2020.

[17] F. Nasr Esfahani, A. Darwish, X. Ma, and P. Twigg, "Non-integrated and integrated on-board battery chargers (iOBCs) for electric vehicles (EVs): A critical review," *Energies*, vol. 17, no. 10, p. 2285, May 2024.

[18] C. Shi, Y. Tang, and A. Khaligh, "A three-phase integrated onboard charger for plug-in electric vehicles," *IEEE Trans. Power Electron.*, vol. 33, no. 6, pp. 4716–4725, Jun. 2018.

[19] T. Na, X. Yuan, J. Tang, and Q. Zhang, "A review of on-board integrated electric vehicles charger and a new single-phase integrated charger," *CPSS Trans. Power Electron. Appl.*, vol. 4, no. 4, pp. 288–298, Dec. 2019.

[20] M. Y. Metwly, M. S. Abdel-Majeed, A. S. Abdel-Khalik, R. A. Hamdy, M. S. Hamad, and S. Ahmed, "A review of integrated on-board EV battery chargers: Advanced topologies, recent developments and optimal selection of FSCW slot/pole combination," *IEEE Access*, vol. 8, pp. 85216–85242, 2020.

[21] S. Sharma, M. V. Aware, and A. Bhowate, "Integrated battery charger for EV by using three-phase induction motor stator windings as filter," *IEEE Trans. Transport. Electrific.*, vol. 6, no. 1, pp. 83–94, Mar. 2020.

[22] S. Semsar, T. Soong, and P. W. Lehn, "On-board single-phase integrated electric vehicle charger with V2G functionality," *IEEE Trans. Power Electron.*, vol. 35, no. 11, pp. 12072–12084, Nov. 2020.

[23] A. Khaligh and M. D'Antonio, "Global trends in high-power on-board chargers for electric vehicles," *IEEE Trans. Veh. Technol.*, vol. 68, no. 4, pp. 3306–3324, Apr. 2019.

[24] G. Rizzoli, M. Mengoni, L. Vancini, G. Sala, A. Tani, and L. Zarri, "Integrated boost-converter for 400 V–800 V fast-charging compatibility," in *Proc. 2nd Int. Conf. Sustain. Mobility Appl., Renewables Technol. (SMART)*, Nov. 2022, pp. 1–8.

[25] J. Gupta, R. Maurya, and S. R. Arya, "Integrated on-board electric vehicle battery charger with multifunctional features," *Austral. J. Electr. Electron. Eng.*, vol. 22, no. 2, pp. 121–139, Apr. 2025.

[26] Y. Xiao, C. Liu, and F. Yu, "An integrated on-board EV charger with safe charging operation for three-phase IPM motor," *IEEE Trans. Ind. Electron.*, vol. 66, no. 10, pp. 7551–7560, Oct. 2019.

[27] Y.-J. Lee, A. Khaligh, and A. Emadi, "Advanced integrated bidirectional AC/DC and DC/DC converter for plug-in hybrid electric vehicles," *IEEE Trans. Veh. Technol.*, vol. 58, no. 8, pp. 3970–3980, Oct. 2009.

[28] X. Zhou, S. Lukic, S. Bhattacharya, and A. Huang, "Design and control of grid-connected converter in bi-directional battery charger for plug-in hybrid electric vehicle application," in *Proc. IEEE Vehicle Power Propuls. Conf.*, Sep. 2009, pp. 1716–1721.

[29] D. Rimpas, S. D. Kaminaris, D. D. Piromalis, G. Vokas, K. G. Arvanitis, and C.-S. Karavas, "Comparative review of motor technologies for electric vehicles powered by a hybrid energy storage system based on multi-criteria analysis," *Energies*, vol. 16, no. 6, p. 2555, Mar. 2023.

[30] S. N. Jani and J. G. Jamnani, "A comparative study of electric motor for low-power density electric vehicles," *Environ. Sci. Pollut. Res.*, vol. 32, no. 22, pp. 13172–13178, Apr. 2023.

[31] X. Liu, J. Hong, B. Sun, W. Zhang, and J. Jiang, "Influence of high-order electromagnetic force on vibration characteristics of induction motor," *IET Electric Power Appl.*, vol. 17, no. 11, pp. 1379–1389, Nov. 2023.

[32] M. Popescu, L. Di Leonardo, G. Fabri, G. Volpe, N. Riviere, and M. Villani, "Design of induction motors with flat wires and copper rotor for E-vehicles traction system," *IEEE Trans. Ind. Appl.*, vol. 59, no. 3, pp. 3889–3900, May 2023.

[33] V. M. Macharia, V. K. Garg, and D. Kumar, "A review of electric vehicle technology: Architectures, battery technology and its management system, relevant standards, application of artificial intelligence, cyber security, and interoperability challenges," *IET Electr. Syst. Transp.*, vol. 13, no. 2, p. 12083, Jun. 2023.

[34] J. D. C. Sousa, T. J. C. Sousa, V. Monteiro, and J. L. Afonso, "Traction system for electric vehicles based on synchronous reluctance permanent magnet machine," *Electronics*, vol. 12, no. 3, p. 539, Jan. 2023.

[35] G. V. Kumar, C.-H. Chuang, M.-Z. Lu, and C.-M. Liaw, "Development of an electric vehicle synchronous reluctance motor drive," *IEEE Trans. Veh. Technol.*, vol. 69, no. 5, pp. 5012–5024, May 2020.

[36] A. Credo, M. Villani, G. Fabri, and M. Popescu, "Adoption of the synchronous reluctance motor in electric vehicles: A focus on the flux weakening capability," *IEEE Trans. Transport. Electrific.*, vol. 9, no. 1, pp. 805–818, Mar. 2023.

[37] Y. Lan, Y. Benomar, K. Deepak, A. Aksoz, M. E. Baghdadi, E. Bostanci, and O. Hegazy, "Switched reluctance motors and drive systems for electric vehicle powertrains: State of the art analysis and future trends," *Energies*, vol. 14, no. 8, p. 2079, Apr. 2021.

[38] M. A. Gaafar, A. Abdelmaksoud, M. Orabi, H. Chen, and M. Dardeer, "Switched reluctance motor converters for electric vehicles applications: Comparative review," *IEEE Trans. Transport. Electrific.*, vol. 9, no. 3, pp. 3526–3544, Sep. 2023.

[39] W. Yan, H. Chen, S. Liao, Y. Liu, and H. Cheng, "Design of a low-ripple double-modular-stator switched reluctance machine for electric vehicle applications," *IEEE Trans. Transport. Electrific.*, vol. 7, no. 3, pp. 1349–1358, Sep. 2021.

[40] M. S. Mastoi, S. Zhuang, H. M. Munir, M. Haris, M. Hassan, M. Usman, S. S. H. Bukhari, and J.-S. Ro, "An in-depth analysis of electric vehicle charging station infrastructure, policy implications, and future trends," *Energy Rep.*, vol. 8, pp. 11504–11529, Nov. 2022.

[41] I. Aretxabaleta, I. M. De Alegria, J. Andreu, I. Kortabarria, and E. Robles, "High-voltage stations for electric vehicle fast-charging: Trends, standards, charging modes and comparison of unity power-factor rectifiers," *IEEE Access*, vol. 9, pp. 102177–102194, 2021.

[42] C. C. Chan and K. T. Chau, "An overview of power electronics in electric vehicles," *IEEE Trans. Ind. Electron.*, vol. 44, no. 1, pp. 3–13, Jan. 1997.

[43] C. H. Dharmakeerthi, N. Mithulananthan, and T. K. Saha, "Overview of the impacts of plug-in electric vehicles on the power grid," in *Proc. IEEE PES Innov. Smart Grid Technol.*, Nov. 2011, pp. 1–8.

[44] R. C. Green, L. Wang, and M. Alam, "The impact of plug-in hybrid electric vehicles on distribution networks: A review and outlook," *Renew. Sustain. Energy Rev.*, vol. 15, no. 1, pp. 544–553, Jan. 2011.

[45] O. C. Onar and A. Khaligh, "Grid interactions and stability analysis of distribution power network with high penetration of plug-in hybrid electric vehicles," in *Proc. 25th Annu. IEEE Appl. Power Electron. Conf. Exposit. (APEC)*, Feb. 2010, pp. 1755–1762.

[46] M. El Chehaly, O. Saadeh, C. Martinez, and G. Joos, "Advantages and applications of vehicle to grid mode of operation in plug-in hybrid electric vehicles," in *Proc. IEEE Electr. Power Energy Conf. (EPEC)*, Oct. 2009, pp. 1–6.

[47] A. K. Karmaker, M. A. Hossain, H. R. Pota, A. Onen, and J. Jung, "Energy management system for hybrid renewable energy-based electric vehicle charging station," *IEEE Access*, vol. 11, pp. 27793–27805, 2023.

[48] F. Ahmad, M. S. Alam, S. M. Shariff, and M. Krishnamurthy, "A cost-efficient approach to EV charging station integrated community microgrid: A case study of Indian power market," *IEEE Trans. Transport. Electrific.*, vol. 5, no. 1, pp. 200–214, Mar. 2019.

[49] S. M. Shariff, M. S. Alam, F. Ahmad, Y. Rafat, M. S. J. Asghar, and S. Khan, "System design and realization of a solar-powered electric vehicle charging station," *IEEE Syst. J.*, vol. 14, no. 2, pp. 2748–2758, Jun. 2020.

[50] *IEEE Recommended Practice and Requirements for Harmonic Control in Electric Power Systems*, IEEE Standard 519-2014 (Revision of IEEE Std 519-1992), Jun. 2014, pp. 1–29. [Online]. Available: https://standards.ieee.org/standard/519-2014.html

[51] M. Nicholas, "Estimating electric vehicle charging infrastructure costs across major U.S. metropolitan areas," Int. Council Clean Transp., Washington, DC, USA, Work. Paper 2019-14, 2019.

[52] M. Smith and J. Castellano, "Costs associated with non-residential electric vehicle supply equipment: Factors to consider in the implementation of electric vehicle charging stations," U.S. Dept. Energy, Washington, DC, USA, Tech. Rep. DOE/EE-1289, Nov. 2015.

[53] Q. Wu, A. H. Nielsen, J. Østergaard, S. T. Cha, and Y. Ding, "Impact study of electric vehicle (EV) integration on medium voltage (MV) grids," in *Proc. 2nd IEEE PES Int. Conf. Exhib. Innov. Smart Grid Technol.*, Dec. 2011, pp. 1–7.

[54] K. Clement-Nyns, E. Haesen, and J. Driesen, "The impact of charging plug-in hybrid electric vehicles on a residential distribution grid," *IEEE Trans. Power Syst.*, vol. 25, no. 1, pp. 371–380, Feb. 2010.

[55] J. McLaren, P. Gagnon, D. Zimny-Schmitt, M. DeMinco, and E. Wilson, "Maximum demand charge rates for commercial and industrial electricity tariffs in the United States," Nat. Renew. Energy Lab., Golden, CO, USA, Tech. Rep. 74, 2017, doi: 10.7799/1392982.

[56] F. Mwasilu, J. J. Justo, E.-K. Kim, T. D. Do, and J.-W. Jung, "Electric vehicles and smart grid interaction: A review on vehicle to grid and renewable energy sources integration," *Renew. Sustain. Energy Rev.*, vol. 34, pp. 501–516, Jun. 2014.

[57] A. Al-Obaidi, H. Khani, H. E. Z. Farag, and M. Mohamed, "Bidirectional smart charging of electric vehicles considering user preferences, peer to peer energy trade, and provision of grid ancillary services," *Int. J. Electr. Power Energy Syst.*, vol. 124, Jan. 2021, Art. no. 106353.

[58] A. Shukla, K. Verma, and R. Kumar, "Impact of EV fast charging station on distribution system embedded with wind generation," *J. Eng.*, vol. 2019, no. 18, pp. 4692–4697, Jul. 2019.

[59] P. Denholm and M. Hand, "Grid flexibility and storage required to achieve very high penetration of variable renewable electricity," *Energy Policy*, vol. 39, no. 3, pp. 1817–1830, Mar. 2011.

[60] S. Seme, N. Lukač, B. Štumberger, and M. Hadžiselimović, "Power quality experimental analysis of grid-connected photovoltaic systems in urban distribution networks," *Energy*, vol. 139, pp. 1261–1266, Nov. 2017.

[61] Q. Zhang, M. Mao, G. Ke, L. Zhou, and B. Xie, "Stability problems of PV inverter in weak grid: A review," *IET Power Electron.*, vol. 13, no. 11, pp. 2165–2174, Aug. 2020.

[62] V. Telukunta, J. Pradhan, A. Agrawal, M. Singh, and S. G. Srivani, "Protection challenges under bulk penetration of renewable energy resources in power systems: A review," *CSEE J. Power Energy Syst.*, vol. 3, no. 4, pp. 365–379, Dec. 2017.

[63] M. Liserre, T. Sauter, and J. Y. Hung, "Future energy systems: Integrating renewable energy sources into the smart power grid through industrial electronics," *IEEE Ind. Electron. Mag.*, vol. 4, no. 1, pp. 18–37, Mar. 2010.

[64] V. Kumar, A. S. Pandey, and S. K. Sinha, "Grid integration and power quality issues of wind and solar energy system: A review," in *Proc. Int. Conf. Emerg. Trends Electr. Electron. Sustain. Energy Syst. (ICETEESES)*, Mar. 2016, pp. 71–80.

[65] B. Battke, T. S. Schmidt, D. Grosspietsch, and V. H. Hoffmann, "A review and probabilistic model of lifecycle costs of stationary batteries in multiple applications," *Renew. Sustain. Energy Rev.*, vol. 25, pp. 240–250, Sep. 2013.

[66] S. Allard, S. Mima, V. Debusschere, T. T. Quoc, P. Criqui, and N. Hadjsaid, "European transmission grid expansion as a flexibility option in a scenario of large scale variable renewable energies integration," *Energy Econ.*, vol. 87, Mar. 2020, Art. no. 104733.

[67] N. S. Pearre and L. G. Swan, "Statistical approach for improved wind speed forecasting for wind power production," *Sustain. Energy Technol. Assessments*, vol. 27, pp. 180–191, Jun. 2018.

[68] P. Louka, G. Galanis, N. Siebert, G. Kariniotakis, P. Katsafados, I. Pytharoulis, and G. Kallos, "Improvements in wind speed forecasts for wind power prediction purposes using Kalman filtering," *J. Wind Eng. Ind. Aerodynamics*, vol. 96, no. 12, pp. 2348–2362, Dec. 2008.

[69] P. Finn and C. Fitzpatrick, "Demand side management of industrial electricity consumption: Promoting the use of renewable energy through real-time pricing," *Appl. Energy*, vol. 113, pp. 11–21, Jan. 2014.

[70] S. M. Hakimi, A. Hasankhani, M. Shafie-Khah, and J. P. S. Catalão, "Demand response method for smart microgrids considering high renewable energies penetration," *Sustain. Energy, Grids Netw.*, vol. 21, Mar. 2020, Art. no. 100325.

[71] T. Harakawa and T. Tujimoto, "Efficient solar power equipment for electric vehicles: Improvement of energy conversion efficiency for charging electric vehicles," in *Proc. IEEE Int. Vehicle Electron. Conf.*, Jun. 2001, pp. 11–16.

[72] M. Etezadi-Amoli, K. Choma, and J. Stefani, "Rapid-charge electric-vehicle stations," *IEEE Trans. Power Del.*, vol. 25, no. 3, pp. 1883–1887, Jul. 2010.

[73] M. Alonso-Abellá and F. Chenlo, "Photovoltaic charging station for electrical vehicles," in *Proc. 3rd World Conf. Photovoltaic Energy Convers.*, vol. 3, May 2003, pp. 2280–2283.

[74] Q. Wang, I. Safak Bayram, F. Granelli, and M. Devetsikiotis, "Fast power charging strategy for EV/PHEV in parking campus with deployment of renewable energy," in *Proc. IEEE 19th Int. Workshop Comput. Aided Model. Design Commun. Links Netw. (CAMAD)*, Dec. 2014, pp. 370–374.

[75] B. Ramachandran, S. K. Srivastava, and D. A. Cartes, "Intelligent power management in micro grids with EV penetration," *Expert Syst. Appl.*, vol. 40, no. 16, pp. 6631–6640, Nov. 2013.

[76] N. Rezaei, A. Khazali, M. Mazidi, and A. Ahmadi, "Economic energy and reserve management of renewable-based microgrids in the presence of electric vehicle aggregators: A robust optimization approach," *Energy*, vol. 201, Jun. 2020, Art. no. 117629.

[77] S. O. Amrouche, D. Rekioua, T. Rekioua, and S. Bacha, "Overview of energy storage in renewable energy systems," *Int. J. hydrogen energy*, vol. 41, no. 45, pp. 20914–20927, 2016.

[78] A. A. Kebede, T. Kalogiannis, J. Van Mierlo, and M. Berecibar, "A comprehensive review of stationary energy storage devices for large scale renewable energy sources grid integration," *Renew. Sustain. Energy Rev.*, vol. 159, May 2022, Art. no. 112213.

[79] K. M. Tan, T. S. Babu, V. K. Ramachandaramurthy, P. Kasinathan, S. G. Solanki, and S. K. Raveendran, "Empowering smart grid: A comprehensive review of energy storage technology and application with renewable energy integration," *J. Energy Storage*, vol. 39, Jul. 2021, Art. no. 102591.

[80] J. Mitali, S. Dhinakaran, and A. A. Mohamad, "Energy storage systems: A review," *Energy Storage Saving*, vol. 1, no. 3, pp. 166–216, Sep. 2022.

[81] M. A. Hannan, S. B. Wali, P. J. Ker, M. S. A. Rahman, M. Mansor, V. K. Ramachandaramurthy, K. M. Muttaqi, T. M. I. Mahlia, and Z. Y. Dong, "Battery energy-storage system: A review of technologies, optimization objectives, constraints, approaches, and outstanding issues," *J. Energy Storage*, vol. 42, Oct. 2021, Art. no. 103023.

[82] S. Thangavel, D. Mohanraj, T. Girijaprasanna, S. Raju, C. Dhanamjayulu, and S. M. Muyeen, "A comprehensive review on electric vehicle: Battery management system, charging station, traction motors," *IEEE Access*, vol. 11, pp. 20994–21019, 2023.

[83] K. Li and K. J. Tseng, "Energy efficiency of lithium-ion battery used as energy storage devices in micro-grid," in *Proc. 41st Annu. Conf. IEEE Ind. Electron. Soc.*, Nov. 2015, pp. 005235–005240.

[84] K. Mongird et al., "Energy storage technology and cost characterization report," Pacific Northwest Nat. Lab., Richland, WA, USA, Tech. Rep. PNNL-28866, 2019. [Online]. Available: https://www.osti.gov/servlets/purl/1573487

[85] M. M. Hoque, M. A. Hannan, and A. Mohamed, "Optimal CC-CV charging of lithium-ion battery for charge equalization controller," in *Proc. Int. Conf. Adv. Electr., Electron. Syst. Eng. (ICAEES)*, Nov. 2016, pp. 610–615.

[86] A. Aghmadi and O. A. Mohammed, "Energy storage systems: Technologies and high-power applications," *Batteries*, vol. 10, no. 4, p. 141, Apr. 2024.

[87] S. Vazquez, S. M. Lukic, E. Galvan, L. G. Franquelo, and J. M. Carrasco, "Energy storage systems for transport and grid applications," *IEEE Trans. Ind. Electron.*, vol. 57, no. 12, pp. 3881–3895, Dec. 2010.

[88] D. P. Dubal, O. Ayyad, V. Ruiz, and P. Gómez-Romero, "Hybrid energy storage: The merging of battery and supercapacitor chemistries," *Chem. Soc. Rev.*, vol. 44, no. 7, pp. 1777–1790, 2015.

[89] P. Keil, M. Englberger, and A. Jossen, "Hybrid energy storage systems for electric vehicles: An experimental analysis of performance improvements at subzero temperatures," *IEEE Trans. Veh. Technol.*, vol. 65, no. 3, pp. 998–1006, Mar. 2016.

[90] B. Sun, T. Dragicevic, F. D. Freijedo, J. C. Vasquez, and J. M. Guerrero, "A control algorithm for electric vehicle fast charging stations equipped with flywheel energy storage systems," *IEEE Trans. Power Electron.*, vol. 31, no. 9, pp. 6674–6685, Sep. 2016.

[91] T. Anno and H. Koizumi, "Double-input bidirectional DC/DC converter using cell-voltage equalizer with flyback transformer," *IEEE Trans. Power Electron.*, vol. 30, no. 6, pp. 2923–2934, Jun. 2015.

[92] A. Nahavandi, M. T. Hagh, M. B. B. Sharifian, and S. Danyali, "A nonisolated multiinput multioutput DC–DC boost converter for electric vehicle applications," *IEEE Trans. Power Electron.*, vol. 30, no. 4, pp. 1818–1835, Apr. 2015.

[93] M. A. Hannan, M. M. Hoque, A. Mohamed, and A. Ayob, "Review of energy storage systems for electric vehicle applications: Issues and challenges," *Renew. Sustain. Energy Rev.*, vol. 69, pp. 771–789, Mar. 2017.

[94] M. A. Hannan, F. A. Azidin, and A. Mohamed, "Hybrid electric vehicles and their challenges: A review," *Renew. Sustain. Energy Rev.*, vol. 29, pp. 135–150, Jun. 2013.

[95] N. Sulaiman, M. A. Hannan, A. Mohamed, E. H. Majlan, and W. R. Wan Daud, "A review on energy management system for fuel cell hybrid electric vehicle: Issues and challenges," *Renew. Sustain. Energy Rev.*, vol. 52, pp. 802–814, Dec. 2015.

[96] Z. Wang, Y. Zhang, S. You, H. Xiao, and M. Cheng, "An integrated power conversion system for electric traction and V2G operation in electric vehicles with a small film capacitor," *IEEE Trans. Power Electron.*, vol. 35, no. 5, pp. 5066–5077, May 2020.

[97] F. Lacressonniere and B. Cassoret, "Converter used as a battery charger and a motor speed controller in an industrial truck," in *Proc. Eur. Conf. Power Electron. Appl.*, 2005, pp. 7 pp.–P.7.

[98] S. Haghbin, S. Lundmark, M. Alakula, and O. Carlson, "An isolated high-power integrated charger in electrified-vehicle applications," *IEEE Trans. Veh. Technol.*, vol. 60, no. 9, pp. 4115–4126, Nov. 2011.

[99] P. Pescetto and G. Pellegrino, "Integrated isolated OBC for EVs with 6-phase traction motor drives," in *Proc. IEEE Energy Convers. Congr. Exposit. (ECCE)*, Oct. 2020, pp. 4112–4117.

[100] I. Subotic, N. Bodo, E. Levi, M. Jones, and V. Levi, "Isolated chargers for EVs incorporating six-phase machines," *IEEE Trans. Ind. Electron.*, vol. 63, no. 1, pp. 653–664, Jan. 2016.

[101] I. Kougioulis, A. Pal, P. Wheeler, and M. R. Ahmed, "An isolated multiport DC–DC converter for integrated electric vehicle on-board charger," *IEEE J. Emerg. Sel. Topics Power Electron.*, vol. 11, no. 4, pp. 4178–4198, Aug. 2023.

[102] P. Pescetto, M. F. T. Cruz, F. Stella, and G. Pellegrino, "Galvanically isolated on-board charger fully integrated with 6-phase traction motor drives," *IEEE Access*, vol. 11, pp. 26059–26069, 2023.

[103] G. T. Chiang, T. Shuji, S. Takahide, Y. Hand, Y. Kitamura, and M. Fukada, "Coupled magnetic-based integrated isolated onboard battery charger and boost motor drive unit for electric vehicles," *IEEE Trans. Transport. Electrific.*, vol. 8, no. 1, pp. 135–148, Mar. 2022.

[104] A. S. Abdel-Khalik, A. Massoud, and S. Ahmed, "Interior permanent magnet motor-based isolated on-board integrated battery charger for electric vehicles," *IET Electric Power Appl.*, vol. 12, no. 1, pp. 124–134, Jan. 2018.

[105] S. Haghbin, S. Lundmark, M. Alakula, and O. Carlson, "Grid-connected integrated battery chargers in vehicle applications: Review and new solution," *IEEE Trans. Ind. Electron.*, vol. 60, no. 2, pp. 459–473, Feb. 2013.

[106] I. Subotic and E. Levi, "A review of single-phase on-board integrated battery charging topologies for electric vehicles," in *Proc. IEEE Workshop Electr. Mach. Design, Control Diagnosis (WEMDCD)*, Mar. 2015, pp. 136–145.

[107] I. Subotic, N. Bodo, and E. Levi, "Single-phase on-board integrated battery chargers for EVs based on multiphase machines," *IEEE Trans. Power Electron.*, vol. 31, no. 9, pp. 6511–6523, Sep. 2016.

[108] D. Thimmesch, "An SCR inverter with an integral battery charger for electric vehicles," *IEEE Trans. Ind. Appl.*, vols. IA–21, no. 4, pp. 1023–1029, Jul. 1985.

[109] D. Bhule and R. S. Kaarthik, "A model predictive control scheme for a single-phase integrated battery charger with active power decoupling for EV application," *IEEE Trans. Power Electron.*, vol. 39, no. 4, pp. 4117–4126, Apr. 2024.

[110] H. Karneddi and D. Ronanki, "A single-phase integrated onboard charger with a wide voltage range for plug-in electric vehicles," in *Proc. IEEE Appl. Power Electron. Conf. Expo. (APEC)*, Feb. 2024, pp. 1288–1293.

[111] C. Shi, Y. Tang, and A. Khaligh, "A single-phase integrated onboard battery charger using propulsion system for plug-in electric vehicles," *IEEE Trans. Veh. Technol.*, vol. 66, no. 12, pp. 10899–10910, Dec. 2017.

[112] S. Ranjith, V. Vidya, and R. S. Kaarthik, "An integrated EV battery charger with retrofit capability," *IEEE Trans. Transport. Electrific.*, vol. 6, no. 3, pp. 985–994, Sep. 2020.

[113] C. Viana, M. Pathmanathan, and P. W. Lehn, "Dual-inverter-integrated three-phase EV charger based on split-phase machine," *IEEE Trans. Power Electron.*, vol. 37, no. 12, pp. 15175–15185, Dec. 2022.

[114] V. F. Pires, J. Monteiro, A. Cordeiro, and J. F. Silva, "Integrated battery charger for electric vehicles based on a dual-inverter drive and a three-phase current rectifier," *Electronics*, vol. 8, no. 10, p. 1199, Oct. 2019.

[115] H. J. Raherimihaja, F. Zhang, T. Na, and Q. Zhang, "An integrated charger using segmented windings of interior permanent magnet motor based on 3 phase with 9 windings," in *Proc. 13th IEEE Conf. Ind. Electron. Appl. (ICIEA)*, May 2018, pp. 565–570.

[116] M. Eull, L. Zhou, M. Jahnes, and M. Preindl, "Bidirectional nonisolated fast charger integrated in the electric vehicle traction drivetrain," *IEEE Trans. Transport. Electrific.*, vol. 8, no. 1, pp. 180–195, Mar. 2022.

[117] M. Z. Farooqi, B. Singh, and B. K. Panigrahi, "Enhanced control and modulation of on-board integrated EV charger with active power decoupling capability," *IEEE Trans. Transport. Electrific.*, vol. 10, no. 4, pp. 8286–8297, Dec. 2024.

[118] H. Karneddi, D. Ronanki, and J. Rodriguez, "Universal integrated onboard charger with model predictive current control for plug-in EV charging," *IEEE Trans. Power Electron.*, vol. 40, no. 1, pp. 28–33, Jan. 2025.

[119] R. A. Taha, W. E. Abdel-Azim, A. Shawier, M. Y. Metwly, A. S. Abdel-Khalik, M. S. Hamad, R. A. Hamdy, S. Gadoue, and S. Ahmed, "Single-phase charging of six-phase integrated on-board battery charger using predictive current control," *IEEE Trans. Transport. Electrific.*, vol. 10, no. 1, pp. 540–552, Mar. 2024.

[120] C. Viana and P. W. Lehn, "A drivetrain integrated DC fast charger with buck and boost functionality and simultaneous drive/charge capability," *IEEE Trans. Transport. Electrific.*, vol. 5, no. 4, pp. 903–911, Dec. 2019.

[121] C. Viana, M. Keshani, and P. W. Lehn, "Interleaved buck-boost integrated DC fast charger with bidirectional fault blocking capability," in *Proc. 20th Workshop Control Model. Power Electron. (COMPEL)*, Jun. 2019, pp. 1–7.

[122] R. Shi, S. Semsar, and P. W. Lehn, "Constant current fast charging of electric vehicles via a DC grid using a dual-inverter drive," *IEEE Trans. Ind. Electron.*, vol. 64, no. 9, pp. 6940–6949, Sep. 2017.

[123] M. A. Khan, I. Husain, and Y. Sozer, "Integrated electric motor drive and power electronics for bidirectional power flow between the electric vehicle and DC or AC grid," *IEEE Trans. Power Electron.*, vol. 28, no. 12, pp. 5774–5783, Dec. 2013.

[124] J. Yang, G. C. Lim, C. Hwang, and J.-I. Ha, "Two-phase DC charging method for improved efficiency and zero torque in motor-integrated charger," *IEEE Trans. Ind. Electron.*, vol. 72, no. 5, pp. 4535–4545, May 2024.

[125] Z. Amjadi and S. S. Williamson, "Power-electronics-based solutions for plug-in hybrid electric vehicle energy storage and management systems," *IEEE Trans. Ind. Electron.*, vol. 57, no. 2, pp. 608–616, Feb. 2010.

[126] H. V. Nguyen, D.-C. Lee, and F. Blaabjerg, "A novel SiC-based multifunctional onboard battery charger for plug-in electric vehicles," *IEEE Trans. Power Electron.*, vol. 36, no. 5, pp. 5635–5646, May 2021.

[127] L. Pan and C. Zhang, "A high power density integrated charger for electric vehicles with active ripple compensation," *Math. Problems Eng.*, vol. 2015, no. 1, 2015, Art. no. 918296.

[128] J. Cai and X. Zhao, "An on-board charger integrated power converter for EV switched reluctance motor drives," *IEEE Trans. Ind. Electron.*, vol. 68, no. 5, pp. 3683–3692, May 2021.

[129] G. Huang, X. Yuan, K. Shi, and X. Wu, "A BP-PID controller-based multi-model control system for lateral stability of distributed drive electric vehicle," *J. Franklin Inst.*, vol. 356, no. 13, pp. 7290–7311, 2019.

[130] J. Saeed, M. Niakinezhad, N. Fernando, and L. Wang, "Model predictive control of an electric vehicle motor drive integrated battery charger," in *Proc. IEEE 13th Int. Conf. Compat., Power Electron. Power Eng. (CPE-POWERENG)*, Apr. 2019, pp. 1–6.

[131] D. Pedrosa, R. Gomes, V. Monteiro, J. C. A. Fernandes, J. Monteiro, and J. L. Afonso, "Model predictive control of an on-board fast battery charger for electric mobility applications," in *Proc. 12th Portuguese Conf. Autom. Control*, 2016, pp. 679–689.

[132] H.-X. Li and H. B. Gatland, "Conventional fuzzy control and its enhancement," *IEEE Trans. Syst., Man Cybern., B (Cybern.)*, vol. 26, no. 5, pp. 791–797, May 1996.

[133] G. Feng, "A survey on analysis and design of model-based fuzzy control systems," *IEEE Trans. Fuzzy Syst.*, vol. 14, no. 5, pp. 676–697, Oct. 2006.

[134] D. Driankov, H. Hellendoorn, and M. Reinfrank, *An Introduction to Fuzzy Control*. Cham, Switzerland: Springer, 2013.

[135] F. De Luca, V. Calderaro, and V. Galdi, "A fuzzy logic-based control algorithm for the recharge/V2G of a nine-phase integrated on-board battery charger," *Electronics*, vol. 9, no. 6, p. 946, Jun. 2020.

[136] S. Ghosh, A. K. Singh, R. Singh, R. Maurya, S. N. Singh, and G. Yang, "Intelligent control of integrated on-board charger with improved power quality and reduced charging transients," *ISA Trans.*, vol. 135, pp. 355–368, Apr. 2023.

[137] A. Hassannia, S. M. Barakati, and S. H. Torabi, "Robust discrete sliding mode controller design for a single-phase onboard integrated electric vehicle charger with disturbance estimation," *Comput. Electr. Eng.*, vol. 110, Sep. 2023, Art. no. 108881.

[138] M. Monfared and S. Golestan, "Control strategies for single-phase grid integration of small-scale renewable energy sources: A review," *Renew. Sustain. Energy Rev.*, vol. 16, no. 7, pp. 4982–4993, Sep. 2012.

[139] S. Golestan, M. Monfared, F. D. Freijedo, and J. M. Guerrero, "Advantages and challenges of a type-3 PLL," *IEEE Trans. Power Electron.*, vol. 28, no. 11, pp. 4985–4997, Nov. 2013.

[140] N. Jaalam, N. A. Rahim, A. H. A. Bakar, C. Tan, and A. M. A. Haidar, "A comprehensive review of synchronization methods for grid-connected converters of renewable energy source," *Renew. Sustain. Energy Rev.*, vol. 59, pp. 1471–1481, Jun. 2016.

[141] T. Cao, Z. Ye, Q. Wu, X. Wan, J. Wang, and D. Li, "A review of adaptive control methods for grid-connected PV inverters in complex distribution systems," *Energies*, vol. 18, no. 3, p. 473, Jan. 2025.

[142] J. Dannehl, C. Wessels, and F. W. Fuchs, "Limitations of voltage-oriented PI current control of grid-connected PWM rectifiers with *LCL* filters," *IEEE Trans. Ind. Electron.*, vol. 56, no. 2, pp. 380–388, Feb. 2009.

[143] S. A. Bonab and A. Emadi, "MPC-based energy management strategy for an autonomous hybrid electric vehicle," *IEEE Open J. Ind. Appl.*, vol. 1, pp. 171–180, 2020.

[144] A. Iovine, T. Rigaut, G. Damm, E. De Santis, and M. D. D. Benedetto, "Power management for a DC MicroGrid integrating renewables and storages," *Control Eng. Pract.*, vol. 85, pp. 59–79, Apr. 2019.

[145] S. P. Chowdhury, S. Chowdhury, and P. A. Crossley, "Islanding protection of active distribution networks with renewable distributed generators: A comprehensive survey," *Electric Power Syst. Res.*, vol. 79, no. 6, pp. 984–992, Jun. 2009.

[146] C. J. Mozina, "Interconnection protection of IPP generators at commercial/industrial facilities," in *Proc. Conf. Rec. IEEE Ind. Appl. Conf., 35th IAS Annu. Meeting World Conf. Ind. Appl. Electr. Energy*, vol. 5, Jun. 2000, pp. 3273–3280.

[147] C. M. Affonso, W. Freitas, W. Xu, and L. C. P. da Silva, "Performance of ROCOF relays for embedded generation applications," *IEE Proc. - Gener., Transmiss. Distrib.*, vol. 152, no. 1, pp. 109–114, 2005.

[148] W. Bower and M. Ropp, "Evaluation of islanding detection methods for utility-interactive inverters in photovoltaic systems," Sandia National Labs., Albuquerque, NM, USA, Tech. Rep. SAND2002-3591, Nov. 2002. [Online]. Available: https://www.osti.gov/servlets/purl/806700

[149] H. H. Zeineldin and J. L. Kirtley, "A simple technique for islanding detection with negligible nondetection zone," *IEEE Trans. Power Del.*, vol. 24, no. 2, pp. 779–786, Apr. 2009.

[150] S. Syamsuddin, N. A. Rahim, Krismadinata, and J. Selvaraj, "Implementation of TMS320F2812 in islanding detection for photovoltaic grid connected inverter," in *Proc. Int. Conf. Tech. Postgraduates (TECHPOS)*, Dec. 2009, pp. 1–5.

[151] A. Çiçek, "Optimal operation of an all-in-one EV station with photovoltaic system including charging, battery swapping and hydrogen refueling," *Int. J. Hydrogen Energy*, vol. 47, no. 76, pp. 32405–32424, Sep. 2022.

[152] A. Çiçek, I. Sengör, S. Güner, F. Karakus, A. K. Erenoglu, O. Erdinç, M. Shafie-Khah, and J. P. S. Catalão, "Integrated rail system and EV parking lot operation with regenerative braking energy, energy storage system and PV availability," *IEEE Trans. Smart Grid*, vol. 13, no. 4, pp. 3049–3058, Jul. 2022.

[153] V. Shah and S. Payami, "Switched reluctance motor drivetrain with fully integrated battery charger and instantaneous zero charging torque for electric transportation," *IEEE Trans. Transport. Electrific.*, vol. 10, no. 2, pp. 4529–4541, Jun. 2024.

[154] Y. Xiao and C. Liu, "A study of rotational movement and charging torque of reconfigured on-board charger," *IEEE Trans. Power Electron.*, vol. 35, no. 10, pp. 10720–10728, Oct. 2020.

[155] A. A. Khan, D. Afriyie, M. Al Saaideh, and S. Ahmed, "A novel and simple integrated on-board charger for e-mobility," *IEEE Trans. Ind. Electron.*, vol. 72, no. 4, pp. 3534–3542, Apr. 2025.

[156] T. Ji, F. Yu, Q. Yin, and X. Liu, "Six-phase drive-based integrated onboard battery charger for electric vehicles considering zero-sequence circulating current elimination," *J. Power Electron.*, vol. 23, no. 3, pp. 478–490, Mar. 2023.

[157] E. Abramushkina, A. Zhaksylyk, T. Geury, M. El Baghdadi, and O. Hegazy, "A thorough review of cooling concepts and thermal management techniques for automotive WBG inverters: Topology, technology and integration level," *Energies*, vol. 14, no. 16, p. 4981, Aug. 2021.

[158] E. Laloya, Ó. Lucía, H. Sarnago, and J. M. Burdío, "Heat management in power converters: From state of the art to future ultrahigh efficiency systems," *IEEE Trans. Power Electron.*, vol. 31, no. 11, pp. 7896–7908, Nov. 2016.

[159] K. Gupta, C. Da Silva, M. Nasr, A. Assadi, H. Matsumoto, O. Trescases, and C. H. Amon, "Thermal management strategies for a high-frequency, bi-directional, on-board electric vehicle charger," in *Proc. 17th IEEE Intersociety Conf. Thermal Thermomechanical Phenomena Electron. Syst. (ITherm)*, May 2018, pp. 935–943.

[160] R. Singh, T. Oridate, and T. Nguyen, "Drive train cooling options for electric vehicles," *Frontiers Heat Mass Transf.*, vol. 22, no. 3, pp. 703–717, 2024.

[161] J. Zachariae, M. Tiesler, R. Singh, T.-A. Benning, and C. Schweikert, "Silicon carbide based traction inverter cooling in electric vehicle using heat pipes," *Thermal Sci. Eng. Prog.*, vol. 46, Dec. 2023, Art. no. 102155.

[162] C. Li, D. Jiao, J. Jia, F. Guo, and J. Wang, "Thermoelectric cooling for power electronics circuits: Modeling and active temperature control," *IEEE Trans. Ind. Appl.*, vol. 50, no. 6, pp. 3995–4005, Nov. 2014.

[163] A. Martinez, D. Astrain, and P. Aranguren, "Thermoelectric self-cooling for power electronics: Increasing the cooling power," *Energy*, vol. 112, pp. 1–7, Oct. 2016.

[164] *Electric Vehicle Conductive Charging System–Part 1: General Requirements*, document IEC 61851-1, I. E. Commission, 2017.

[165] *Protection Against Electric Shock-common Aspects for Installation and Equipment*, document IEC 61140, International Electrotechnical Committee, 2001.

[166] *Methods of Measurement of Touch Current and Protective Conductor Current*, document IEC 60990, International Electrotechnical Commission, 2016.

[167] R. Gaska, Q. Chen, J. Yang, A. Osinsky, M. Asif Khan, and M. S. Shur, "High-temperature performance of AlGaN/GaN HFETs on SiC substrates," *IEEE Electron Device Lett.*, vol. 18, no. 10, pp. 492–494, Oct. 1997.

[168] J. Palumbo, O. Tayyara, S. A. Assadi, C. M. Da Silva, O. Trescases, C. H. Amon, and S. Chandra, "Implementation of a topologically optimized heat sink for non-uniform heat fluxes in an electric-vehicle fast-charger," in *Proc. 22nd IEEE Intersociety Conf. Thermal Thermomechanical Phenomena Electron. Syst. (ITherm)*, May 2023, pp. 1–8.

[169] G. S. Sodhi, C. Botting, E. Lau, M. Palanisamy, M. Rouhani, and M. Bahrami, "Hybrid heat sinks for thermal management of passively cooled battery chargers," *Int. J. Energy Res.*, vol. 45, no. 4, pp. 6333–6349, Mar. 2021.

[170] B. Al-Hanahi, I. Ahmad, D. Habibi, P. Pradhan, and M. A. S. Masoum, "An optimal charging solution for commercial electric vehicles," *IEEE Access*, vol. 10, pp. 46162–46175, 2022.

[171] K. Kozielski, G. A. Mudiyanselage, M. Narimani, and A. Emadi, "A review of three-port integrated on-board charger and auxiliary power module in electric medium- and heavy-duty vehicles," *IEEE Open J. Power Electron.*, vol. 6, pp. 1347–1370, 2025.

[172] P. Franzese, D. D. Patel, A. A. S. Mohamed, D. Iannuzzi, B. Fahimi, M. Risso, and J. M. Miller, "Fast DC charging infrastructures for electric vehicles: Overview of technologies, standards, and challenges," *IEEE Trans. Transport. Electrific.*, vol. 9, no. 3, pp. 3780–3800, Sep. 2023.

[173] S. Valedsaravi, A. El Aroudi, and L. Martínez-Salamero, "Review of solid-state transformer applications on electric vehicle DC ultra-fast charging station," *Energies*, vol. 15, no. 15, p. 5602, Aug. 2022.

[174] Y. Tahir, I. Khan, S. Rahman, M. F. Nadeem, A. Iqbal, Y. Xu, and M. Rafi, "A state-of-the-art review on topologies and control techniques of solid-state transformers for electric vehicle extreme fast charging," *IET Power Electron.*, vol. 14, no. 9, pp. 1560–1576, Jul. 2021.

[175] A. C. Nair and B. G. Fernandes, "A solid state transformer based fast charging station for all categories of electric vehicles," in *Proc. 44th Annu. Conf. IEEE Ind. Electron. Soc.*, Oct. 2018, pp. 1989–1994.

[176] E. I. Pool-Mazun, J. J. Sandoval, P. N. Enjeti, and I. J. Pitel, "An integrated solid-state transformer with high-frequency isolation for EV fast-charging applications," *IEEE J. Emerg. Sel. Topics Ind. Electron.*, vol. 1, no. 1, pp. 46–56, Jul. 2020.

[177] J. Millán, P. Godignon, X. Perpiña, A. Pérez-Tomás, and J. Rebollo, "A survey of wide bandgap power semiconductor devices," *IEEE Trans. Power Electron.*, vol. 29, no. 5, pp. 2155–2163, May 2014.

[178] E. A. Jones, F. F. Wang, and D. Costinett, "Review of commercial GaN power devices and GaN-based converter design challenges," *IEEE J. Emerg. Sel. Topics Power Electron.*, vol. 4, no. 3, pp. 707–719, Sep. 2016.

[179] J. V. P. S. Chennu, R. Maheshwari, and H. Li, "New resonant gate driver circuit for high-frequency application of silicon carbide MOSFETs," *IEEE Trans. Ind. Electron.*, vol. 64, no. 10, pp. 8277–8287, Oct. 2017.

[180] D. Han, S. Li, W. Lee, and B. Sarlioglu, "Adoption of wide bandgap technology in hybrid/electric vehicles-opportunities and challenges," in *Proc. IEEE Transp. Electrific. Conf. Expo (ITEC)*, Jun. 2017, pp. 561–566.

[181] H. A. Mantooth, M. D. Glover, and P. Shepherd, "Wide bandgap technologies and their implications on miniaturizing power electronic systems," *IEEE J. Emerg. Sel. Topics Power Electron.*, vol. 2, no. 3, pp. 374–385, Sep. 2014.

[182] T. Kitamura, M. Yamada, S. Harada, and M. Koyama, "Development of high-power density interleaved DC/DC converter with SiC devices," *Electr. Eng. Jpn.*, vol. 196, no. 3, pp. 22–29, Aug. 2016.

[183] U.S. Department of Energy. (Feb. 2015). *Wide Bandgap Power Electronics Technology Assessment*. [Online]. Available: https://www.energy.gov/sites/prod/files/2015/02/f19/QTR%20Ch8%20-%20Wide%20Bandgap%20TA%20Feb-13-2015.pdf

[184] S. Saxena, L. Kong, and M. G. Pecht, "Exploding E-cigarettes: A battery safety issue," *IEEE Access*, vol. 6, pp. 21442–21466, 2018.

[185] X.-Y. Yao, L. Kong, and M. G. Pecht, "Reliability of cylindrical Li-Ion battery safety vents," *IEEE Access*, vol. 8, pp. 101859–101866, 2020.

[186] H. Lee, B. Y. Shin, S. Han, S. Jung, B. Park, and G. Jang, "Compensation for the power fluctuation of the large scale wind farm using hybrid energy storage applications," *IEEE Trans. Appl. Supercond.*, vol. 22, no. 3, pp. 5701904, Jun. 2012.

[187] A. A. Khodadoost Arani, G. B. Gharehpetian, and M. Abedi, "A novel control method based on droop for cooperation of flywheel and battery energy storage systems in islanded microgrids," *IEEE Syst. J.*, vol. 14, no. 1, pp. 1080–1087, Mar. 2020.

[188] S. Esther, S. K. Singh, A. K. Goswami, and N. Sinha, "Recent challenges in vehicle to grid integrated renewable energy system: A review," in *Proc. 2nd Int. Conf. Intell. Comput. Control Syst. (ICICCS)*, Jun. 2018, pp. 427–435.

[189] P. Purkait, M. Basu, and S. R. Nath, "Renewable energy integration to electric power grid: Opportunities, challenges, and solutions," in *Challenges and Opportunities of Distributed Renewable Power* (Energy, Environment, and Sustainability). Singapore: Springer, 2024, pp. 37–100. [Online]. Available: https://link-springer-com.recursos.biblioteca.upc.edu/chapter/10.1007/978-981-97-1406-3_3

[190] K. M. Tan, V. K. Ramachandaramurthy, and J. Y. Yong, "Integration of electric vehicles in smart grid: A review on vehicle to grid technologies and optimization techniques," *Renew. Sustain. Energy Rev.*, vol. 53, pp. 720–732, Jan. 2016.

[191] D. Mazzeo, N. Matera, R. De Luca, and R. Musmanno, "A smart algorithm to optimally manage the charging strategy of the home to vehicle (H2V) and vehicle to home (V2H) technologies in an off-grid home powered by renewable sources," *Energy Syst.*, vol. 15, no. 2, pp. 715–752, May 2024.

[192] Y. Park, O. C. Onar, and B. Ozpineci, "Potential cybersecurity issues of fast charging stations with quantitative severity analysis," in *Proc. IEEE Cyber PELS (CyberPELS)*, Knoxville, TN, USA, 2019, pp. 1–7, doi: 10.1109/CyberPELS.2019.8925069.

[193] D. Li, M.-F. Leung, J. Tang, Y. Wang, J. Hu, and S. Wang, "Generative self-supervised learning for cyberattack-resilient EV charging demand forecasting," *IEEE Trans. Intell. Transp. Syst.*, early access, Feb. 27, 2025, doi: 10.1109/TITS.2025.3545577.

[194] D. Li, J. Tang, B. Zhou, P. Cao, J. Hu, M.-F. Leung, and Y. Wang, "Toward resilient electric vehicle charging monitoring systems: Curriculum guided multi-feature fusion transformer," *IEEE Trans. Intell. Transp. Syst.*, vol. 25, no. 12, pp. 21356–21366, Dec. 2024.

[195] W. Wang, F. H. Memon, Z. Lian, Z. Yin, T. R. Gadekallu, Q.-V. Pham, K. Dev, and C. Su, "Secure-enhanced federated learning for AI-empowered electric vehicle energy prediction," *IEEE Consum. Electron. Mag.*, vol. 12, no. 2, pp. 27–34, Mar. 2023.

[196] A. Miglani and N. Kumar, "Blockchain-based co-operative caching for secure content delivery in CCN-enabled V2G networks," *IEEE Trans. Veh. Technol.*, vol. 72, no. 4, pp. 5274–5289, Apr. 2023.

[197] Z. Wan, T. Zhang, W. Liu, M. Wang, and L. Zhu, "Decentralized privacy-preserving fair exchange scheme for V2G based on blockchain," *IEEE Trans. Dependable Secure Comput.*, vol. 19, no. 4, pp. 2442–2456, Jul. 2022.

[198] Y. Zhang, J. Zou, and R. Guo, "Efficient privacy-preserving authentication for V2G networks," *Peer-Peer Netw. Appl.*, vol. 14, no. 3, pp. 1366–1378, May 2021.

[199] P. Prabawa and D.-H. Choi, "Distributionally robust PV planning and curtailment considering cyber attacks on electric vehicle charging under PV/load uncertainties," *Energy Rep.*, vol. 11, pp. 3436–3449, Jun. 2024.

[200] M. Kumar, U. Dohare, S. Kumar, and N. Kumar, "Blockchain based optimized energy trading for E-mobility using quantum reinforcement learning," *IEEE Trans. Veh. Technol.*, vol. 72, no. 4, pp. 5167–5180, Apr. 2023.

[201] G. Kumar, R. Saha, M. K. Rai, W. J. Buchanan, R. Thomas, G. Geetha, T. Hoon-Kim, and J. J. P. C. Rodrigues, "A privacy-preserving secure framework for electric vehicles in IoT using matching market and signcryption," *IEEE Trans. Veh. Technol.*, vol. 69, no. 7, pp. 7707–7722, Jul. 2020.

MALIK QAMAR ABBAS (Student Member, IEEE) received the bachelor's degree from The University of Lahore, in 2013, and the master's degree in electrical engineering from COMSATS University, Pakistan, in 2017. He is currently pursuing the Ph.D. degree with the Department of Electrical, Electronic, and Information Engineering "Guglielmo Marconi," University of Bologna. He was a Research Assistant with COMSATS University, for about two years, focusing on the design and implementation of multilevel inverters, bidirectional converters, power supplies, and the control of power converters. Further, he was an Electrical Engineer and had extensive experience supervising and managing wind power plant operations. His research includes, but is not limited to, electrical drives, motor control, and converter design and control.

LASSI AARNIOVUORI (Senior Member, IEEE) received the M.Sc. degree in electrical engineering and the D.Sc. degree in electric motors and drives from Lappeenranta University of Technology (LUT), Lappeenranta, Finland, in 2005 and 2010, respectively. From 2017 to 2019, he was a Marie Curie Fellow with the School of Engineering and Applied Science, Aston University, Birmingham, U.K. He is currently an Associate Professor of electric transportation with the LUT School of Energy Systems. His current research interests include all aspects related to electric transportation systems, especially wide band-gap power switches, high-speed machine technology, modulation methods, simulation of electric drives, efficiency measurements, and calorimetric measurement systems.

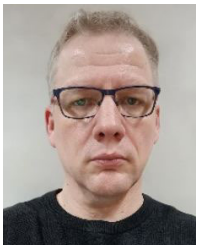

PASI PELTONIEMI (Senior Member, IEEE) received the D.Sc. degree in electrical engineering from LUT University, Finland, in 2010. From 2010 to 2014, he was a Postdoctoral Researcher with the Laboratory of Control Engineering and Digital Systems, LUT University. In 2019, he started as an Associate Professor (tenure track) of power electronics, and in 2023, he became a Full Professor with the Laboratory of Electrical Drives Technology, LUT University. He is currently the Head of the Laboratory of Electrical Drives Technology. His research interests include wide bandgap power electronics, power electronics for electrical drives, grid connected converters, DC grids, and P2X systems.

MICHELE MENGONI (Senior Member, IEEE) received the M.Sc. (Hons.) and Ph.D. degrees in electrical engineering from the University of Bologna, Bologna, Italy, in 2006 and 2010, respectively. He is currently an Associate Professor with the Department of Electrical, Electronic, and Information Engineering "Guglielmo Marconi," University of Bologna. His research interests include the design, analysis, and control of three phase electric machines, multiphase drives, and ac/ac matrix converters. He is an Associate Editor of IEEE TRANSACTIONS ON INDUSTRIAL ELECTRONICS and IEEE TRANSACTIONS ON INDUSTRY APPLICATIONS.

LUCA ZARRI (Senior Member, IEEE) received the M.Sc. and Ph.D. degrees in electrical engineering from the University of Bologna, Bologna, Italy, in 1998 and 2007, respectively. He is currently a Full Professor of power electronics, electrical machines, and drives with the Department of Electrical, Electronic, and Information Engineering "Guglielmo Marconi," University of Bologna. He has authored or co-authored more than 200 scientific articles. His research interests include the control of power converters and electric drives. He is a Senior Member of the IEEE Industry Applications, the IEEE Power Electronics, and the IEEE Industrial Electronics Societies. He is also serving as the Vice Chair for the IEEE IAS Industrial Power Conversion Systems Department.